JGR Atmospheres

RESEARCH ARTICLE
10.1029/2023JD039935

Thermal Response of Large Seasonally Ice-Covered Lakes Over Tibetan Plateau to Climate Change

Yang Wu[1], Anning Huang[2], Xin Li[1], Lijuan Wen[3], Lazhu[4], and Jingyi Li[5]

[1]Nanjing Joint Institute for Atmospheric Sciences, CMA Key Laboratory of Transportation Meteorology, Nanjing, China, [2]School of Atmospheric Sciences, Nanjing University, Nanjing, China, [3]Qinghai Lake Comprehensive Observation and Research Station, Northwest Institute of Eco-Environment and Resources, Chinese Academy of Sciences, Lanzhou, China, [4]Research Center for Ecology, School of Ecology and Environment, Tibet University, Lhasa, China, [5]Nanjing Institute of Geography and Limnology, Chinese Academy of Sciences, Nanjing, China

Abstract In this study, a process-based lake model is used to investigate the influence of climate change on the thermodynamics of 30 large lakes over Tibetan Plateau (TP). The lake model was driven by the atmospheric forcing derived from the bias-corrected projections of three global climate models in the twenty-first century under three Shared Socioeconomic Pathways (SSPs). The hindcasts during 2000–2014 can reasonably capture the seasonality and magnitude of satellite retrieved lake surface temperature (LST). Future projections during 2015–2100 suggest a widespread increased LST, declined ice cover, and prolonged stratification, with the severity of changes in line with the climate driver shifts under different SSPs. Under the scenario with the highest level of anthropogenic radiative forcing (SSP5-8.5), the end-of-century (2086–2100) changes of LST, ice thickness, and stratification duration averaged across all studied lakes reach 4.90°C, −0.43 m, and 65.46 days, respectively. Note that the positive ice-albedo feedback can cause excess lake warming by accelerating ice break-up (30.07 days earlier) and stratification onset (46.83 days earlier). By the end of this century, more frequent, multi-seasonal thermal extremes are anticipated to push nearly half of the studied lakes into a permanent heatwave state. Together with the remarkable LST increase and winter ice loss, the lakes will mix less frequently and may shift from a dimictic to warm monomict mixing regime. Hopefully, the irreversible thermal changes can be avoided if the anthropogenic radiative forcing is controlled within the envelope outlined by the stringent climate mitigation scenario SSP1-2.6.

Plain Language Summary Lake thermodynamics play a fundamental role in controlling a wide range of physical and biogeochemical processes within lakes, for example, evaporation, nutrients and dissolved gases cycling, zooplankton and phytoplankton proliferation. This study uses lake numerical modeling to understand how climate change will affect the thermodynamics of 30 large lakes over TP, examining simulations throughout the twenty-first century under three SSPs. From 2000 to 2014 to 2086–2100, LST increase, ice loss, and stratification prolongation are anticipated across all studied lakes. These changes are more severe under the scenario with higher levels of climate driver shifts. Under the worst scenario SSP5-8.5, the above end-of-century changes reach 4.90°C, −0.43 m, and 65.46 days, respectively. Additionally, by 2100, nearly half of the studied lakes will be in a constant state of "heatwave", meaning the water will be unusually warm all the time. The substantial lake warming and ice loss further cause the lakes to mix less frequently and risk shifts from a dimictic to warm monomict mixing regime. On a hopeful note, the thermal changes can possibly be controlled within the natural envelope if we adhere to the stringent climate mitigation scenario SSP1-2.6.

Key Points:

- Lake numerical modeling gains insights on the large-lake thermal response to a changing climate over TP during the twenty-first century
- Results from the worst scenario project substantial end-of-century changes of LST, thermal extreme, ice, stratification, and mixing regime
- Out-of-control thermal response can be avoided by adhering to the stringent climate mitigation scenario

Supporting Information:

Supporting Information may be found in the online version of this article.

Correspondence to:

A. Huang,
anhuang@nju.edu.cn

Citation:

Wu, Y., Huang, A., Li, X., Wen, L., Lazhu, & Li, J. (2024). Thermal response of large seasonally ice-covered lakes over Tibetan Plateau to climate change. *Journal of Geophysical Research: Atmospheres*, *129*, e2023JD039935. https://doi.org/10.1029/2023JD039935

Received 12 SEP 2023
Accepted 29 MAR 2024

Author Contributions:

Conceptualization: Yang Wu, Anning Huang
Data curation: Yang Wu, Anning Huang, Xin Li, Lijuan Wen, Jingyi Li
Formal analysis: Yang Wu, Anning Huang
Funding acquisition: Yang Wu, Anning Huang, Lijuan Wen
Investigation: Yang Wu, Anning Huang, Xin Li, Lijuan Wen
Methodology: Yang Wu, Anning Huang
Software: Yang Wu, Anning Huang
Supervision: Yang Wu, Anning Huang
Validation: Yang Wu, Anning Huang
Visualization: Yang Wu, Anning Huang
Writing – original draft: Yang Wu, Anning Huang
Writing – review & editing: Yang Wu, Anning Huang, Xin Li, Jingyi Li

1. Introduction

The Tibetan Plateau (TP), known as the "Earth's Third Pole" and "Water Tower of Asia" (Qiu, 2008), is one of the most sensitive regions to global climate change. According to the multi-source observations from meteorological stations and ice cores, the overall climate has been experiencing notable changes of surface warming, air moistening, solar dimming, and wind stilling since the 1980s (Chen et al., 2015; Kuang & Jiao, 2017; Yang et al., 2014). The recent warming rate during 1980–2018 is 0.44°C·decade^{-1} over TP, which is more than twofold that observed globally (0.14°C·decade^{-1}) during 1961–2015 (Zhang et al., 2020). These climate changes have far reaching implications on the widely and densely distributed seasonally ice-covered lakes over TP. Documented impacts have been found in lake number (Tao et al., 2020), area (Tong et al., 2016; Zhang et al., 2019), water level

(Chen & Liao, 2020; Lei et al., 2021), water storage (Qiao et al., 2019; Yang et al., 2017), and thermodynamics (Cai et al., 2022; Xie et al., 2022). Given the seasonality of lake thermodynamics, for example, ice cover, water temperature, and stratification, forms the foundation controlling a wide range of lake physical and biogeochemical processes (Feng et al., 2021; Maberly et al., 2020), understanding the lake thermal response to climate change is of particular importance for effective management and adaptation strategies to protect the fragile aquatic ecosystem and the livelihoods of species dependent on the lakes over TP.

Lakes are commonly regarded as sentinels of climate change (Adrian et al., 2009). Within the recent decades, ice cover loss and lake warming have been widely observed globally (O'Reilly et al., 2015; Sharma et al., 2019; Wang et al., 2021), for example, 2 weeks decrease of ice duration and 1.5°C increase of lake surface temperature (LST) for the global lakes from 1981 to 1990 until 2010–2019 (Grant et al., 2021). The responses to anthropogenic climate warming are much more pronounced for seasonally ice-covered lakes located at middle-latitude or high-altitude regions (Huang et al., 2022; Li et al., 2022; Vinnå et al., 2021). For example, LST of the Great Lakes and large European Lakes has risen more rapidly than the ambient air temperatures due to the positive ice-albedo feedback and joint contributions from other atmospheric variations (Niedrist et al., 2018; Schneider & Hook, 2010). The increased LST would cause reduced water oxygen solubility and prolonged stable thermal stratification, both of which facilitate to exacerbate lake hypoxia and the severity of hypolimnetic oxygen depletion (O'Reilly et al., 2003). Widespread deoxygenation has been found among 393 temperate lakes during 1941–2017, with its mean declined rate being 2.75 to 9.3 times greater than that observed in global oceans (Jane et al., 2021). This further rises concerns about decreased internal nutrient loading and primary productivity (Swann et al., 2020), adverse thermal habitat changes for aquatic organisms (Kraemer et al., 2021), intensified cyanobacterial blooms (Ho et al., 2019; Paerl & Huisman, 2008), and increased production/emission of methane and toxic metal ions (Davison, 1981; Li & Xue, 2021). In addition to the water temperature, lake ice, thermal stratification, and mixing regimes are also crucial factors in determining the nutrient cycling, dissolved oxygen, methane emission, light availability, and thus have knock-on impacts on the biogeochemical processes and species phenology (Merz et al., 2023; Woolway et al., 2022). These consequences of lake thermodynamic changes are already taking place and threaten the socioeconomic functioning and aquatic biodiversity among lake systems worldwide (Verburg et al., 2003; Woolway et al., 2020).

Acknowledging the significance, the generation of various datasets has been actively promoted, including continuous in situ hydrological observations (Qu et al., 2012; Wang, 2020) and both active/passive microwave and multispectral satellite remote sensing (Liu et al., 2019; Qiu et al., 2019; Wan et al., 2017). These efforts have facilitated advancements in monitoring the lake-air interactions and interannual variations in LST and lake ice phenology (Zhang et al., 2020). However, while valuable, first-hand in situ observations are only for short periods and collected on a few large lakes. Satellite observations, typically extending back only to the early 1980s, are constrained by the spatiotemporal resolution, cloud cover, and complex terrain (Guo et al., 2018), rendering them inadequate to address the correspondence between climate change and lake thermal variations over TP. In this context, lake physical models serve as effective tools for understanding the lake-thermal response to climate change. Numerical modeling researches to date have revealed that since the 1970s, rapid changes in air temperature, radiation and wind speed over TP elicited varying thermal responses in lakes such as Qinghai Lake, Lake Nam Co, Ngoring and Garying, indicating the spatial heterogeneity of climate sensitivity (Huang et al., 2017; Kirillin et al., 2017; Shi et al., 2022; Su et al., 2019). However, previous simulation studies mainly concentrate on several large lakes during periods close to the satellite observation era, with scant attention to changes of lake thermal extremes, thermal stratification, and mixing regimes and future variations. Given the prevalence of large seasonally ice-covered lakes over TP, a comprehensive understanding of how various thermal elements of these lakes respond under different future climate change scenarios is of paramount importance for ecological conservation and in formulating policies to preserve the biodiversity of lake ecosystems. In this regard, we aim to address the question by selecting 30 large lakes over TP, each with an area exceeding or near 300 km^2, and investigating their thermal response to a changing climate. The analysis is based on one-dimensional lake simulations forced by the bias-corrected output from three global climate models (GCM) under three Shared Socioeconomic Pathways during the twenty-first century (2000–2100). Main findings will offer valuable insights for researchers and policymakers in understanding the lake thermodynamic variations over TP and coping with related risks on ecosystem, water resource, and aquatic biodiversity.

In the remaining parts of this paper, after introducing the materials and methods (Section 2), model performance will be verified in Section 3. The model analyses will be carried out to investigate the climate-related lake thermal

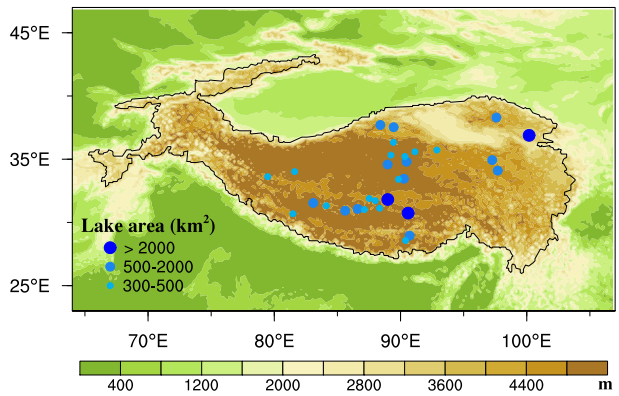

Figure 1. Spatial distribution of land topography (unit: m) and 30 selected large lakes (solid cycles, with the marker sizes denoting magnitude of lake areas) over Tibetan Plateau (TP). The black solid line denotes the TP boundary with an elevation of 3,000 m.

changes in LST, lake heatwave, ice, warm thermal stratification, and mixing regime (Section 4). Main findings of this study as well as the discussion and recommendations for future studies will be provided in Section 5.

2. Material and Methods

2.1. Study Area

Figure 1 shows the geographic location of selected 30 large lakes over TP. The selected lakes range 28.57–38.29°°N in latitude, 79.48 to 100.19°°E in longitude, 3,876–5,010 m in elevation above sea level, 293.5–4,226.2 km^2 in surface area, 4.1–120.0 m in mean depth, and 0–14.7 g·L^{-1} in salinity. The lake names, locations, surface areas, elevation and mean depth are from Guo et al. (2021), and the lake salinity refers Zhu (2021). Details of the lake attributes and datasets are provided in Table 1 and Section 2.2.

2.2. Datasets

The in situ and satellite-derived datasets, as well as the bias-corrected GCM projections, are listed as follows:

(1) An integrated dataset of daily lake-wide mean LST, as well as the name, location, surface area, elevation and mean depth, for 160 lakes across TP (https://doi.org/10.5281/zenodo.5111400, Guo et al., 2021). Note that the LST is the average of water surface temperature and ice surface temperature, weighted with the lake ice area coverage fraction. The dataset includes daytime, nighttime, and daily mean LST during 2000–2017 retrieved from MOD11A1, and also reconstructed daily mean LST during a longer phase of 1978–2017 based on a modified Air2Water model developed by Piccolroaz et al. (2013). Air2Water is a semi-physical model that calculates LST principally based on air temperature according to the lake surface heat balance. It is proved to be an effective tool in obtaining long-term historic LST variations of lakes with different morphology and climatic backgrounds. The satellite-based and model-based LST are comparable and have been well verified with two satellite-based LST datasets released by Layden et al. (2015) and Liu et al. (2019). In present study, this integrated dataset is chosen for validating the performance of one-dimensional lake model in reproducing LST.

(2) Long-term lake ice phenology data of 132 lakes (each with an area exceeding 40 km^2) across TP from 1978 to 2016 (https://figshare.com/articles/dataset/TPLIP/18852338, Wu et al., 2022). The dataset is produced by combining the strengths of remote sensed LST (MOD11A2), snow cover (MOD10A1), and numerical modeling (Air2Water), and includes six phenological indictors, that is, freeze-up start date, freeze-up end date, break-up start date, break-up end, completely ice-duration and ice duration. The dataset has been verified against available in situ records of three lakes, and proved to show high consistency with two satellite-based datasets released by Qiu et al. (2017) and Cai et al. (2019). In this study, freeze-up start date, break-up end, and ice duration are chosen for validation the model performance in replicating ice phenology.

(3) In situ lake water quality parameters of 124 closed lakes over TP (https://doi.org/10.11888/Geogra.tpdc.271450, Zhu, 2021). The selected parameters in this study include the lake water transparency (i.e., Secchi disk depth, Z_{SD}, unit in m) and salinity, which are used for deriving the light extinction coefficient (η, unit in m^{-1}) and parameterizing salinity effects on water thermal properties (to be discussed in Section 2.3).

Finally, three bias-corrected GCM projections, that is, GFDL-ESM4, IPSL-CM6A-LR and MPI-ESM1-2-HR from the Inter-Sectoral Impact Model Intercomparison Project phase 3b (ISIMIP3b, https://www.isimip.org/protocol/3/, Lange & Büchner, 2021), are utilized to drive the one-dimensional lake model. The selected ISIMIP3b datasets with the horizontal resolution of 0.5° × 0.5° include daily surface downward shortwave ($SW_{\downarrow}$) and longwave ($LW_{\downarrow}$) radiation, surface air pressure (PA), 2-m air temperature (T_{2m}), surface specific humidity (SPH), and 10-m wind speed (WS_{10m}) during historic (2000–2014) and future (2015–2100) phases under three SSPs, that is, SSP1-2.6, SSP3-7.0 and SSP5-8.5. The ISIMIP3b data closest to the lake center of each studied lake are extracted to create the meteorological forcings. The future projections encompass a range of low, medium and high future radiative forcings from multiple GCMs, aiming to account for uncertainties in simulating the lake thermal variations. Figures 2 and 3 show the temporal and spatial variations of over-lake atmospheric forcings

Table 1
Attributes of All Studied Lakes, Ranked According to Decreasing Surface Area (Fourth Column)

Lake name	Latitude (°N)	Longitude (°E)	Area (km^2)	Elevation (m)	Mean depth (m)	Salinity (g/L)	η (m^{-1})	α_{imax} (−)
Qinghai	36.89	100.19	4,226.24	3,194	20	14.7	0.15	0.42
Serling Co	31.81	88.99	2,306.48	4,530	28	8	0.292	0.4
Nam Co	30.74	90.60	2,021.71	4,718	45	1.7	0.08	0.55
Ayakkuh	37.53	89.45	1,002.04	3,876	10	-	0.359	0.4
Zhari Namco	30.93	85.62	1,001.59	4,613	25	11	0.25	0.2
Tangra Yumco	31.07	86.61	857.6	4,528	120	9.86	0.1	0.2
Ngoring	34.91	97.70	662.31	4,269	17.6	0.3	0.283	0.4
Ulan UL	34.80	90.47	654.33	4,854	6.9	10.9	0.12	0.5
Har	38.29	97.59	606.93	4,077	27.4	-	0.234	0.4
Migriggyang-zham Co	33.46	90.27	570.58	4,931	25.7	-	0.241	0.4
Yamdrok	28.96	90.72	570.38	4,441	28.2	1.4	0.12	0.45
Aqqik Kol	37.08	88.40	553.28	4,250	9.8	10	0.198	0.3
Gyaring	34.93	97.26	539.9	4,292	8.9	0.5	0.378	0.5
Ngangla- Ringco	31.54	83.09	535.16	4,715	10	-	0.359	0.2
Dogai Coring	34.58	88.97	529.25	4,814	22.5	-	0.85	0.3
Bangong Co	33.62	79.48	499.99	4,241	41.3	0.5	0.25	0.3
Dorsoidong Co	33.41	89.84	494.88	4,921	20	11.6	0.171	0.4
Taro Co	31.14	84.12	485.02	4,566	34.1	0.5	0.1	0.2
Xijir Ulan	35.21	90.34	474.01	4,769	4.7	-	0.322	0.4
Gyaring Co	31.12	88.34	473.14	4,650	32.1	0.2	0.12	0.4
Ngangzi Co	31.02	87.13	465	4,683	8.7	6.6	0.3	0.2
Mapam Yumco	30.68	81.47	411.71	4,586	46	0.2	0.188	0.6
Dogaicoring QangCo	35.32	89.23	396.82	4,787	6.4	-	0.2	0.4
Lumaqangdong Co	34.02	81.61	391.87	4,810	45.1	14.7	0.149	0.4
Hoh Xil	35.59	91.14	354.25	4,878	12.6	9.1	0.1	0.6
Urru Co	31.72	88.00	343.39	4,548	19.2	0.3	0.13	0.2
Jingyu	36.33	89.44	341.79	4,708	4.1	10	0.11	0.5
Hoh Sai	35.72	92.88	316.74	4,475	16.6	-	0.29	0.4
Dogze Co	31.89	87.52	314.15	4,459	8.5	14.69	0.1	0.3
Pumoyong Co	28.57	90.40	292.51	5,010	36.4	0.2	0.208	0.6

Note. Note that η and α_{imax} denote the light extinction coefficient and maximum ice albedo, respectively.

during the twenty-first century. A consistent pattern of decreasing $SW_{\downarrow}$ and WS_{10m}, increasing $LW_{\downarrow}$, total downward radiation $TR_{\downarrow}$(calculated as the sum of $SW_{\downarrow}$ and $LW_{\downarrow}$), T_{2m}, and SPH can be found across all studied lakes and GCM ensembles. The magnitude of multi-GCM averaged changes of atmospheric forcings under SSP1-2.6, SSP3-7.0, and SSP5-8.5 evidently diverges since 2050 and increases more rapidly with the severity of SSP scenario (Figure 2). Under the most stringent scenario SSP1-2.6, the atmospheric forcings show a somewhat end-of-century stabilization, whereas under the medium-high radiative forcing scenarios, they show significant long-term variations. For example, under the worst scenario SSP5-8.5, $SW_{\downarrow}$, $LW_{\downarrow}$, $TR_{\downarrow}$, T_{2m}, SPH, and WS_{10m} averaged over all studied lakes show a long-term significant trend of -1.27 ± 0.05 $W{\cdot}m^{-2}$ $decade^{-1}$, 3.53 ± 0.07 $W{\cdot}m^{-2}$ $decade^{-1}$, 2.25 ± 0.05 $W{\cdot}m^{-2}$ $decade^{-1}$, 0.71 ± 0.02°$C{\cdot}decade^{-1}$, 0.21 ± 0.01 $g{\cdot}kg^{-1}$ $decade^{-1}$, -0.03 ± 0.00 $m{\cdot}s^{-1}$ $decade^{-1}$, with the end-of-century change (2086–2100 minus 2000–2014) at -10.76 $W{\cdot}m^{-2}$, 27.13 $W{\cdot}m^{-2}$, 16.37 $W{\cdot}m^{-2}$, 5.42°C, 1.64 $g{\cdot}kg^{-1}$, and -0.23 $m{\cdot}s^{-1}$, respectively (Figure 3). Given that PA has no direct or clear effect on lake thermodynamics and its end-of-century change is

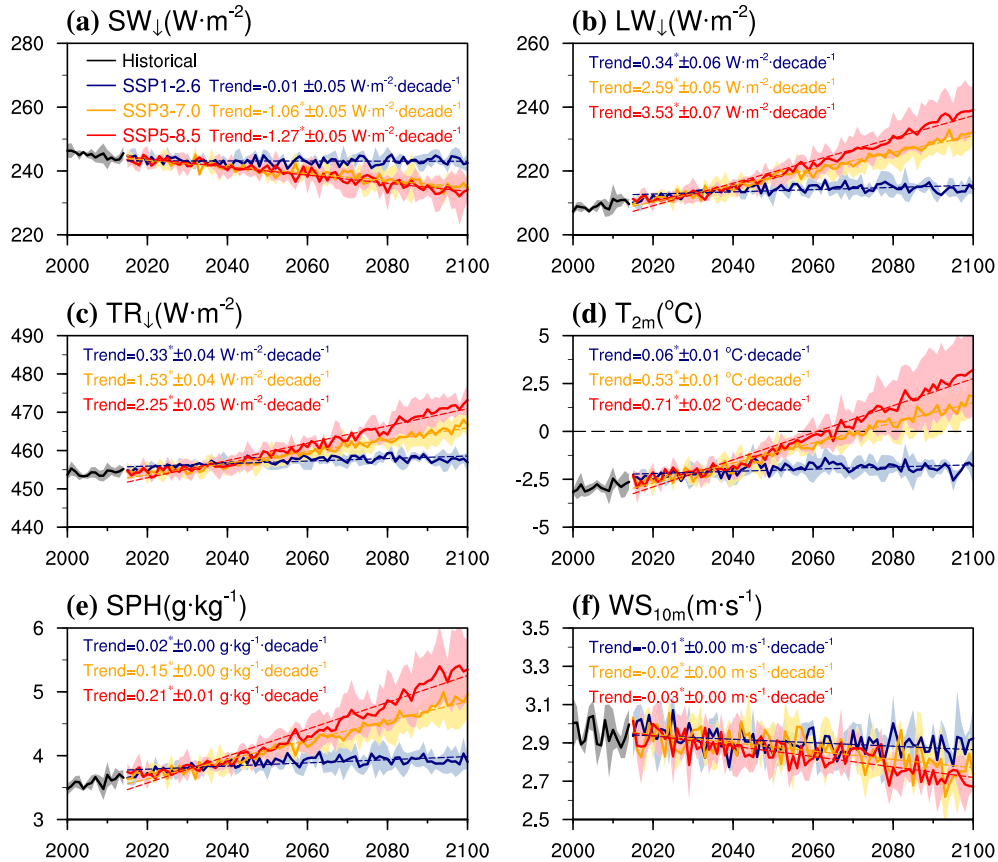

Figure 2. Time series of annual surface (a) downward shortwave ($SW_{\downarrow}$), (b) downward longwave ($LW_{\downarrow}$), (c) downward total radiation ($TR_{\downarrow} = SW_{\downarrow}+LW_{\downarrow}$), (d) 2-m air temperature (T_{2m}), (e) specific humidity (SPH), and (f) 10-m wind speed (WS_{10m}) averaged over all studied lakes during historic (2000–2014) and future (2015–2100) phases. The thick lines denote the mean across three GCM-based forcings, the shaded regions denote standard deviation, and the texts and dashed lines denote long-term trends during 2015–2100. The superscript asterisk of long-term trend indicates its statistical significance at the 0.05 level.

rather small (0.89, 4.33, and 5.63 hPa for SSP1-2.6, SSP3-7, and SSP5-8,5) relative to the climatic mean of 570 hPa, it is excluded in the subsequent analysis.

2.3. Model Description and Experimental Design

The one-dimensional lake model used in this study is referred as offline WRF-Lake, which is a 1-D mass and energy balance model based on the eddy thermal diffusion theory (Henderson-Sellers, 1985; Henderson-Sellers & Davies, 1989; Hostetler & Bartlein, 1990). Offline WRF-Lake is vertically discretized by up to 5 snow layers on lake ice, 25 layers of lake water/ice, and 10 bottom sediment layers, and decently solves the primary physics governing turbulent and diffusive energy transfer at the lake-air interface and lake column. The model is well calibrated by Subin et al. (2012) and Gu et al. (2015), and its applicability on reproducing the seasonality and long-term variability of lake thermodynamics over TP has been extensively tested (Huang et al., 2019; Ma et al., 2022; Shi et al., 2022). Lake model details are described in Wu et al. (2020), with modifications in adding a dynamic parameterization for surface roughness length and reducing the depth-dependent light extinction coefficient η by scaling 0.8. Additionally, when the observed Z_{SD} is available from Zhu (2021), η is determined based on the empirical equations proposed by Bukata et al. (1988) and Poole and Atkins (1929):

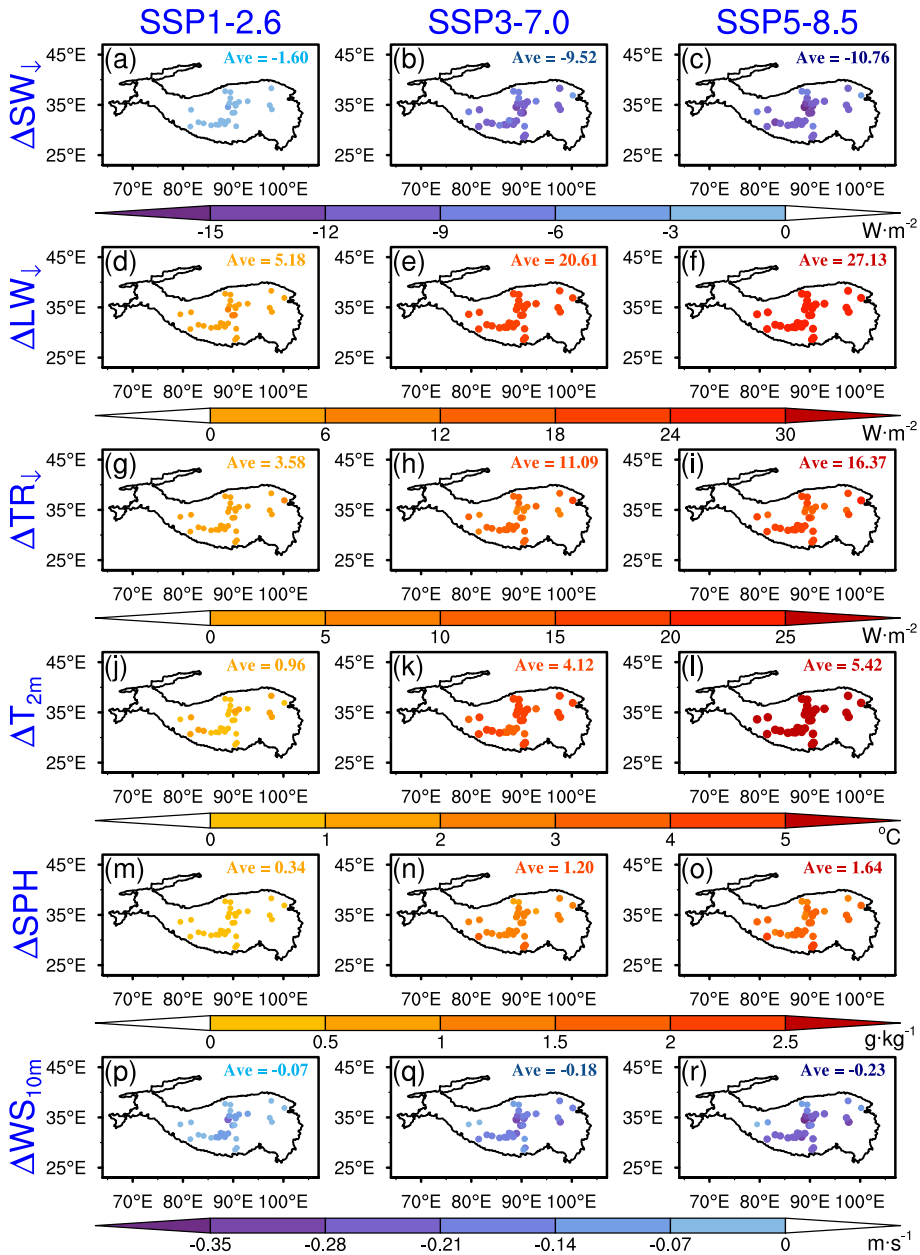

Figure 3. Spatial distributions of the relative change in atmospheric forcings by the end of twenty-first century (2086–2100 minus 2000–2014). Ave denotes the average across all studied lakes.

$$\eta = \begin{cases} \dfrac{0.757}{Z_{SD}} + 0.07 & Z_{SD} \in (2, 10) \\ \dfrac{1.7}{Z_{SD}} & Z_{SD} < 2 \ or \ Z_{SD} > 10 \end{cases} \quad (1)$$

Considering most of the studied lakes are saline, we incorporate a parameterization of salinity effects on water physical properties, for example, the temperature of maximal water density (*Tdmax*, Chen & Millero, 1986), freezing point (Millero, 1978), specific heat capacity (Sun et al., 2008), and thermal conductivity (Wen et al., 2015; Yusufova et al., 1975) into offline WRF-Lake:

$$Tdmax = 3.9839 - 1.9911 \times 10^{-2} PA - 5.822 \times 10^{-6} PA^2 - \left(0.2219 + 1.106 \times 10^{-4} PA\right) S \quad (2)$$

$$T_{fsw} = -0.0575S + 1.710523 \times 10^{-3} S^{1.5} - 2.154996 \times 10^{-4} S^2 \quad (3)$$

$$C_{psw} = C_{pw} - 4.4S \quad (4)$$

$$\lambda_{sw} = \lambda_w \left(1 - 2.2 \times 10^{-2} S + 1 \times 10^{-4} S^2\right) \quad (5)$$

where PA is the surface air pressure (in bar), S is the lake salinity (in $g \cdot L^{-1}$), T_{fsw} is the freezing point for saline water (in °C), C_{psw} (C_{pw}) is the heat capacity for saline (fresh) water (in $J \cdot kg^{-1} \cdot K^{-1}$), and λ_{sw} (λ_w) is the thermal conductivity for saline (fresh) water (in $W \cdot m^{-1}\ K^{-1}$).

On the basis of preliminary work (Huang et al., 2021; Layden et al., 2016), certain lake-specific model parameters, for example, η and maximum ice albedo (α_{imax}), need to be further tuned to achieve reliable modeling of thermodynamics for each lake. Here, we perform a series of parameter-tuning simulations running from 20th May 1999 to 31st December 2014, covering the whole historic phase of 2000–2014. The simulations for 30 selected lakes are done one-by-one and respectively initialized with zero ice cover and a uniform lake column temperature based on the LST from Guo et al. (2021) on 20th May 1999. The atmospheric forcings are updated daily with ISIMIP3b data. The criterion that daily absolute mean bias between the modeled and observed LST during 2000–2014 is less than 1.5°C is adopted for an optimal simulation. The values of lake-specific model parameters are thus determined, as listed in Table 1, and then used for the twenty-first century simulations forced by a collection of three GCMs under three scenarios. We take the model results in 1999 as a spin up phase and use the results from 2000 onward for the following evaluation and analysis.

2.4. Analysis Methodology

Lake heatwave (LHW) is defined as an anomalously warm event lasting for at least five days, during which the LST exceeds the 90th percentile threshold (LST_{90}) of baseline phase (chosen as 2000–2014 in this study). The seasonally varying LST_{90} and baseline climatology LST (LST_{clim}) are calculated based on the daily LST within an 11-day window centered on the day of year across the 15-year baseline phase, as formulated by the methods in Hobday et al. (2016, 2018):

$$LST_{90} = P_{90}\{LST(y, d) | y \in [2000, 2014], d \in [j-5, j+5]\} \quad (6)$$

$$LST_{clim} = \sum_{y=2000}^{2014} \sum_{d=j-5}^{j+5} \frac{LST(y, d)}{11 * 15} \quad (7)$$

where y and d are the year and day of year, respectively. Both calculated LST_{90} and LST_{clim} are smoothed by applying a 31-day moving average. In common with atmospheric heatwaves, two discrete LHW events with a gap of less than 3 days will be considered as a continuous event. In analyzing each LHW event, we focus on two basic metrics, that is, duration (number of days between the start and end dates) and intensity (mean temperature anomaly relative to LST_{clim}, namely $\overline{LST - LST_{clim}}$). Moreover, an intensity-based method is adopted to classify moderate, strong, severe, and extreme LHW categories. Moderate, strong, severe, and extreme events are those LHW with (LST-LST_{clim})/(LST_{90}-LST_{clim}) ranging [1, 2), [2, 3), [3, 4), and [4,∞), respectively. Finally, the annual mean duration and intensity of LHW, and the total annual count of days belonging to each of the defined LHW categories are derived for analysis.

Following Layden et al. (2015) and Woolway, Sharma, et al. (2021), we use LST as a proxy to determine both the ice and warm thermal stratification phenology. That is, the ice onset (break-up) is defined as the first (last) date when LST is below (above) T_{fsw}, and the duration is the total number of days between them. The warm stratification onset (break-up) is defined as the first (last) date when LST is above (below) $Tdmax$, and the duration is the total number of days between them.

The Pearson temporal correlation (TC) and mean bias (BIAS) are used for model evaluation. Specifically, TC ranges −1 to 1, with higher absolute value indicating greater temporal similarity between observation and

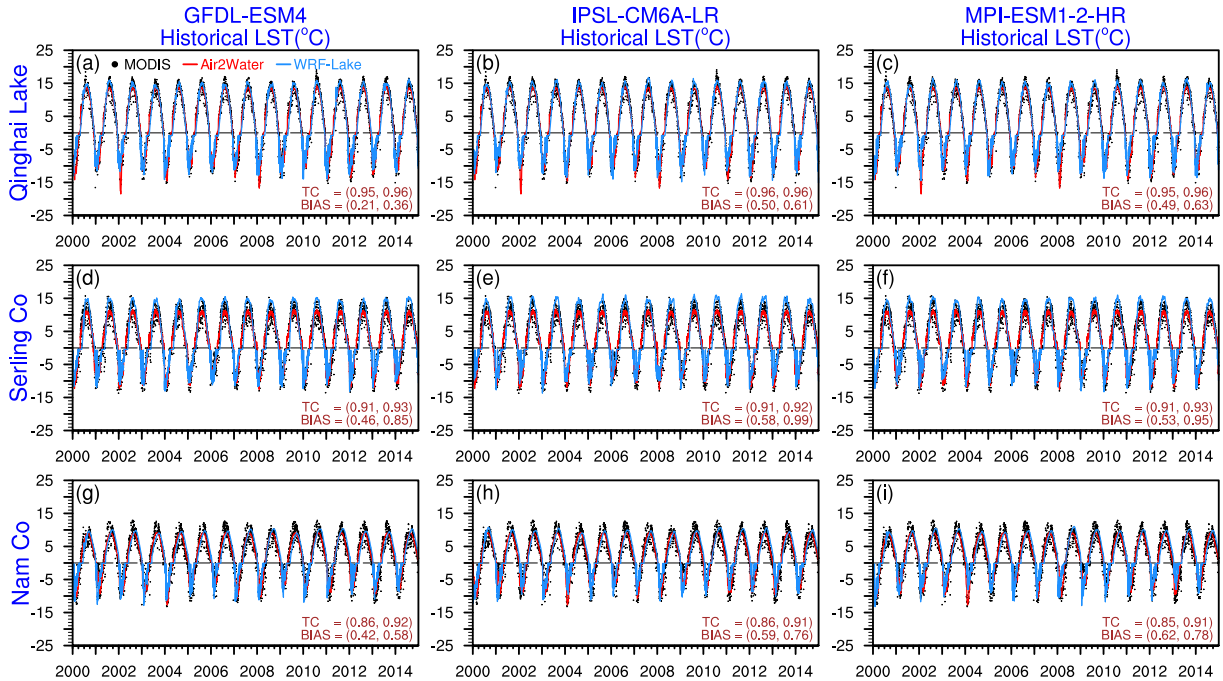

Figure 4. Daily lake surface temperature (LST) at (a)–(c) Qinghai Lake, (d)–(f) Lake Serling Co, and (g)–(i) Lake Nam Co during historic phase (2000–2014) from both MODIS and Air2water products released by Guo et al. (2021) and the offline WRF-Lake simulations driven by three GCM-based atmospheric forcings. The statistics in parentheses are calculated from simulations relative to MODIS and Air2Water, respectively.

simulation. Lower absolute BIAS indicates that the simulated values are more consistent with the observed values in quantity. Details about the statistical formulation can be found in Wu et al. (2019). We define winter as from December to the following February, spring as March to May, summer as June to August, and autumn as September to November. The statistical significance of the linear regression and correlation coefficients is evaluated using the two-tailed Student's *t*-test (Brownlee, 1965).

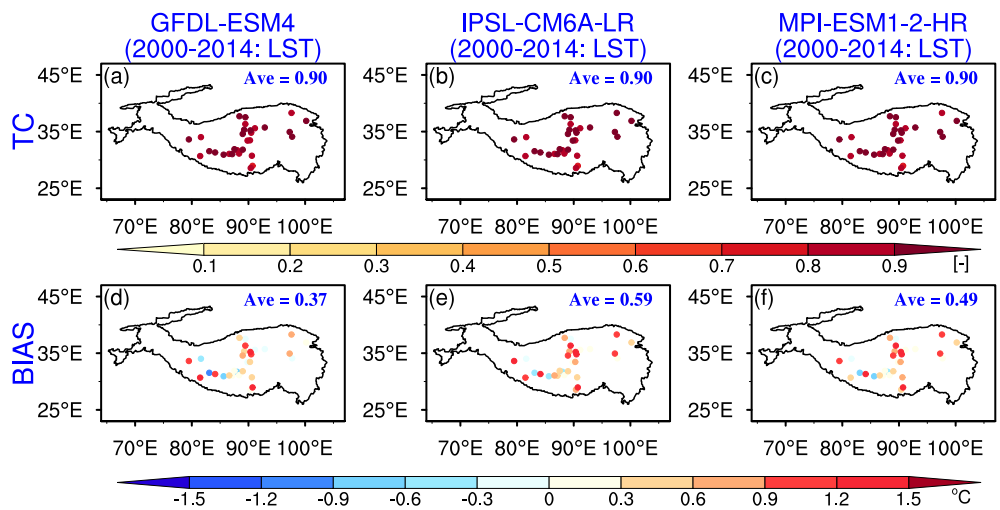

Figure 5. Spatial distributions of evaluation metrics for daily LST from offline WRF-Lake simulations driven by three GCM-based atmospheric forcings relative to MODIS observations. Ave denotes the average of evaluation metrics across all studied lakes.

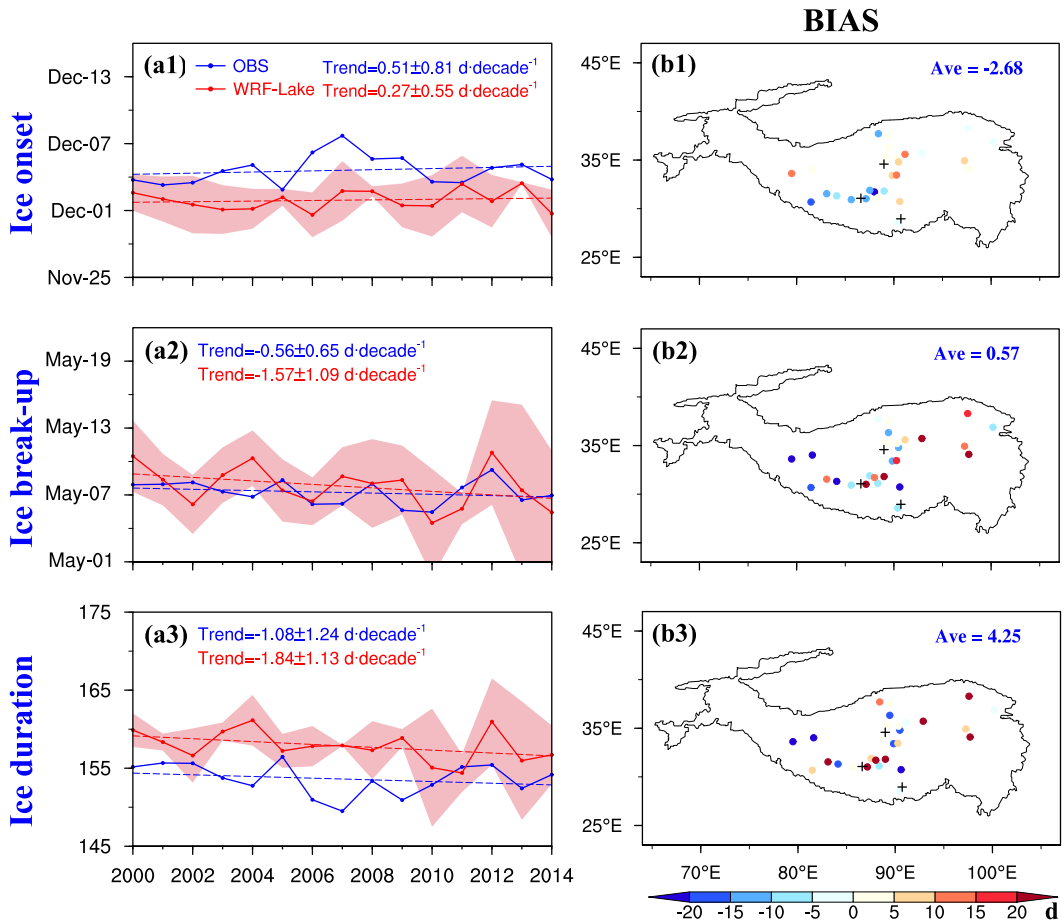

Figure 6. Left column: interannual variations (solid lines) and trends (dashed lines) of (a1) ice onset, (a2) break-up, and (a3) duration averaged over 27 studied lakes during 2000–2014 from observations and the mean across three GCM-based simulations, with the shaded regions denoting the standard deviation. Right column: spatial distributions of BIAS between observations and ensemble mean simulations, with Ave denoting the average of evaluation metrics across lakes. Note that: (a) three lakes, as represented by the black crosses in (b1)–(b3), are excluded from this assessment due to the lack of observations; (b) the short-term interannual trends are not statistically significant.

3. Model Evaluation

Figure 4 compares the daily LST time series of three largest TP lakes from both MODIS and Air2water products released by Guo et al. (2021) with the offline WRF-Lake simulations driven by three GCM-based atmospheric forcings during historic phase (2000–2014). Figure 5 shows the TC and BIAS for daily LST from simulations relative to the MODIS observations across all studied lakes.

From Figure 4, Qinghai Lake, Lake Serling Co, and Lake Nam Co are typical seasonally ice-covered dimictic lakes: (a) The lakes are ice-covered for 4–5 months during cold seasons, with the MODIS (Air2Water) LST of −6.79 (−7.42)°C, −5.84 (−6.29)°C, −2.15 (−2.74)°C in winter and 0.10 (0.75)°C, −0.31 (0.20)°C, −2.26 (−2.69)°C in spring, respectively; (b) The lakes are stratified for 4–5 months during warm seasons, with the MODIS (Air2Water) LST of 12.87 (12.12)°C, 10.28 (9.79)°C, 7.39 (7.27)°C in summer and 8.33 (8.53)°C, 7.53 (6.66)°C, 7.11 (8.80)°C in autumn, respectively. The three GCM-based simulations all reasonably reproduce the observed seasonal evolution of LST, with a mean TC of 0.95 (0.96), 0.91 (0.93), 0.86 (0.91), and BIAS of 0.40 (0.53)°C, 0.52 (0.93)°C, 0.54 (0.71)°C relative to MODIS (Air2Water) for Qinghai Lake, Lake Serling Co, and Lake Nam Co, respectively. Offline WRF-Lake also shows good performance in simulating the temporal evolution and magnitude of LST among all studied lakes, yielding a mean TC of 0.88 and BIAS of 0.48°C relative to MODIS (Figure 5) and a mean TC of 0.93 and BIAS of 0.92°C relative to Air2Water (figure omitted) across three-GCM based simulations. After checking the monthly LST and its magnitude of interannual variation between

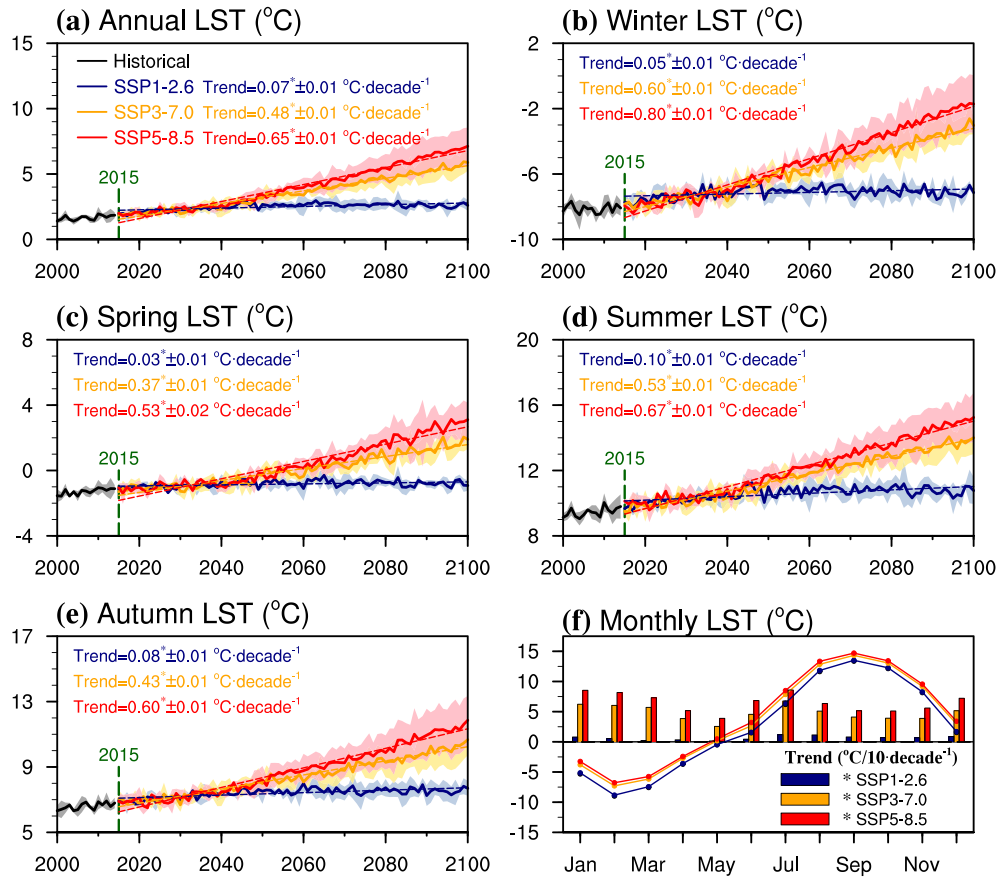

Figure 7. Interannual variations of the (a) annual and (b)–(e) seasonal mean LST averaged over all studied lakes during historic (2000–2014) and future (2015–2100) phases. The thick lines denote the mean across three GCM-based simulations, the shaded regions denote standard deviation, and the texts and dashed lines denote interannual trends during 2015–2100. (f) Monthly LST time series during 2015–2100, with the bars denoting the trends of respective annual time series for each month. The long-term trends are all statistically significant at the 0.05 level and marked with asterisks.

MODIS and model simulations across all studied lakes (Figure S1 in Supporting Information S1), the high TC in Figures 4 and 5 is primarily contributed by the reasonable simulation of seasonal LST variations. Considering that the satellite-retrieved LST over TP is usually lower than the in situ observed values by 0.8–1.9°C due to the cool skin effects (Hook et al., 2003; Ke & Song, 2014), the model BIAS is likely very small and the model can reasonably replicate actual LST values.

Next, we assess the model's performance in simulating the lake ice phenology during historic phase, as depicted in Figure 6. It should be noted that three lakes, namely Lake Tangra Yumco, Lake Yamdrok, and Lake Dogai Coring are excluded from this assessment due to the lack of observational data. According to the observations, lake ice typically forms in early December and persists until early May during 2000–2014 (Figures 6a1–6a3). The mean values of ice onset, break-up, and duration across 27 lakes are 5th December, 7th May, and 154 days, respectively. The lake ice phenology exhibits interannual trends featured by delayed freezing (0.51 ± 0.81 d·decade^{-1}), advanced thawing (-0.56 ± 0.65 d·decade^{-1}), and shortened duration (-1.08 ± 1.24 d·decade^{-1}). The modeled climatological features of lake ice onset, break-up, and duration agree well with observations, with the BIAS of −2.68, 0.57, and 4.25 days averaged over 27 lakes (Figures 6b1–6b3). Moreover, the model replicates the shortening lake ice duration with an interannual trend of -1.84 ± 1.13 d·decade^{-1}, albeit with some overestimation. Overall, the offline WRF-Lake model can reasonably reproduce the ice phenology of large lakes over TP, making it suitable for studying their long-term response to future climate change.

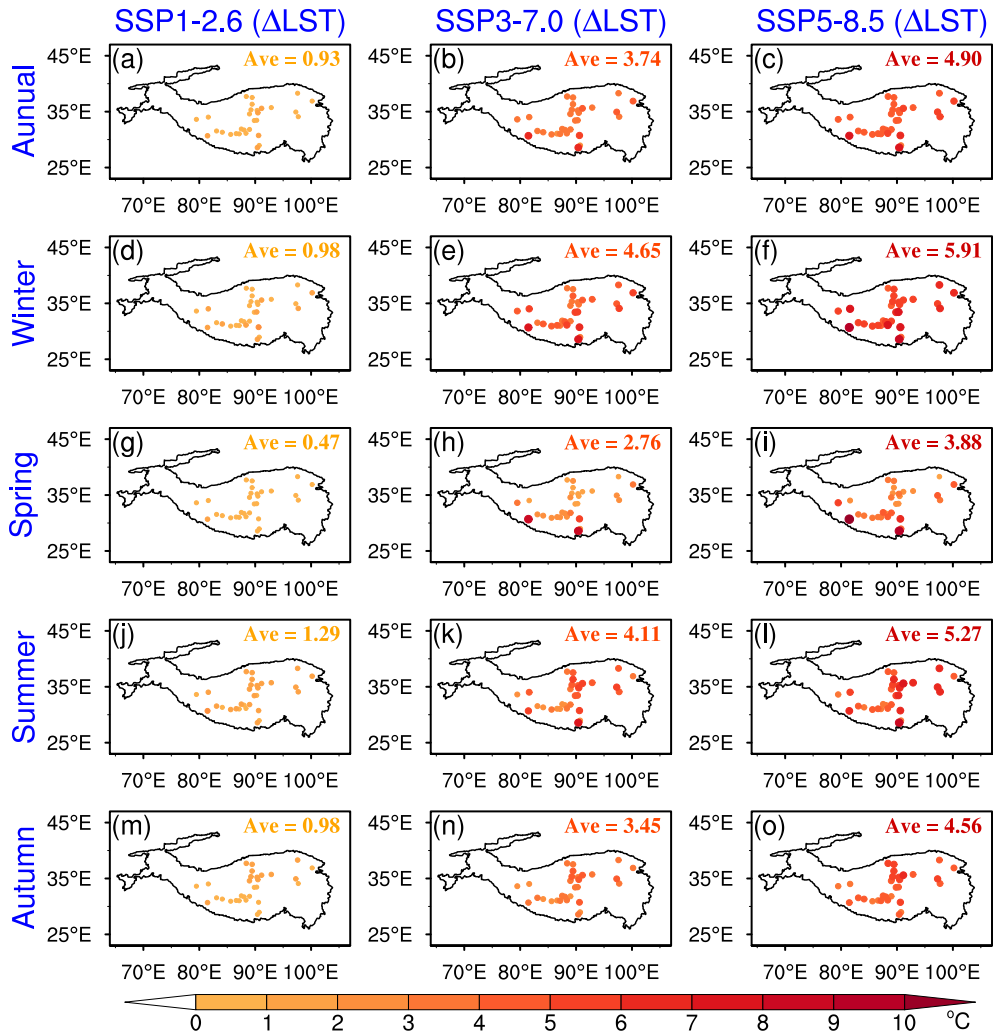

Figure 8. Spatial distributions of the relative change in (a)–(c) annual and (d)–(o) seasonal LST (unit: °C) by the end of twenty-first century (2086–2100 minus 2000–2014). Ave denotes the average across all studied lakes.

4. Lake Thermal Response to Climate Change

4.1. LST

Figure 7 shows the interannual variations of annual and seasonal LST averaged over all studied lakes during 2000–2100, with the end-of-century LST changes shown in Figure 8. The three-GCM based projections reveal a consistent upward trend for the annual and seasonal LST, and the trend and end-of-century increase of LST are much more pronounced under medium-high radiative forcing scenarios (Figures 7a–7e and 8). The LST during winter and summer months shows stronger rising trends and end-of-century increases (Figures 7f and 8). On average, the end-of-century increase of annual LST across 30 lakes is 4.90°C under SSP5-8.5, with relatively larger increase of 5.91 and 5.27°C for LST during winter and summer. This is likely caused by the changes of lake ice and thermal stratification. Specifically, during winter months, a decreased areal fraction of lake ice cover corresponds to a decrease in surface albedo, favoring more extensive absorption of incident radiation and LST increase. During summer months, the stable warm thermal stratification restricts vertical turbulent mixing, and the volume of surface water participating directly in the lake-air interactions is smaller, causing higher sensitivity of surface water temperature to meteorological variations.

In scenarios SSP3-7.0 and SSP5-8.5, the mean projected trends of annual LST are 0.48 ± 0.01 and 0.65 ± 0.01° C·decade^{-1} (significance at the 0.05 level), respectively, reaching 90.57% and 91.54% of the concurrent air temperature rise (Figures 3d and 7a). The relatively modest increase scale of LST compared with air temperature

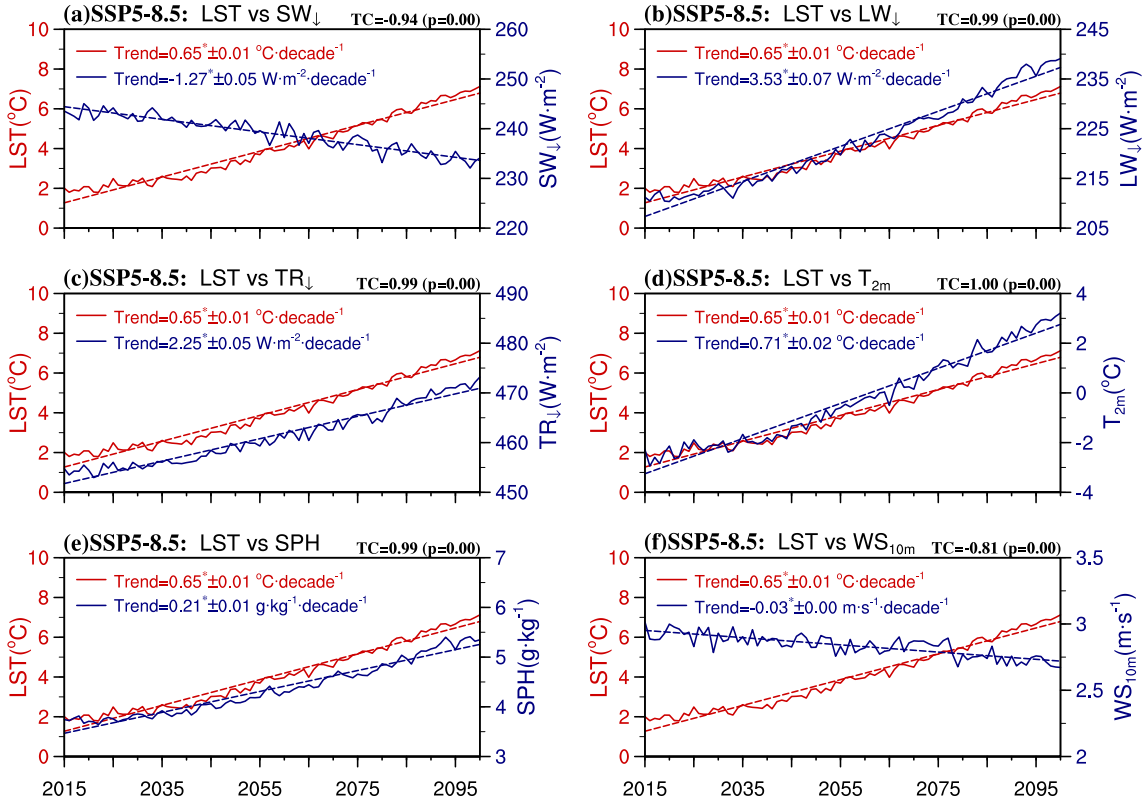

Figure 9. Interannual variations (solid lines) and trends (dashed lines) of LST and atmospheric forcing variables under SSP5-8.5 during 2015–2100. All results are based on the average across all studied lakes. The long-term trends are all statistically significant at the 0.05 level and marked with asterisks.

(+0.9°C·°C_{air}^{-1}) was also reported by Grant et al. (2021) based on the global-scale lake thermal projections across future climate scenarios. This phenomenon is anticipated since the LST increase is muted by the loss of additional energy related to enhanced evaporative cooling and emitted longwave radiation (Wang et al., 2018; Woolway et al., 2020). However, four lakes, namely Lake NamCo, Mapam Yumco, Hoh Xil, and Pumoyong, are predicted to warm faster than the ambient air. For example, Lake Mapam Yumco has a warming rate of 0.85 (1.11) °C·decade^{-1} under SSP3-7.0 (SSP5-8.5), which is 1.49 (1.44) times the ambient air warming rates. This indicates that the climate factors driving LST increase, such as rising T_{2m}, increasing $TR_{\downarrow}$, rising *SPH*, and decreasing WS_{10m} (Figure 3), along with the local amplification effects due to reduced lake ice cover and enhanced thermal stratification exhibit somewhat spatial heterogeneity.

Next, we examine the relationship between LST and atmospheric forcing variables under SSP5-8.5 during 2015–2100 (Figure 9). The projected long-term LST increase is significantly correlated with the interannual variations of $SW_{\downarrow}$, $LW_{\downarrow}$, $TR_{\downarrow}$, T_{2m}, *SPH*, and WS_{10m}, with the TC of −0.94, 0.99, 0.99, 1.00, 0.99, and −0.81, respectively. Note that the strong linear relationship does not imply causality. From the perspective of lake surface energy budget, higher downward radiation and T_{2m} correspond to more energy input on lake surface. Increased *SPH* and decreased WS_{10m} act to weaken the surface turbulent heat loss and vertical mixing. Thus, the weakening $SW_{\downarrow}$ has a negative impact on LST increase, while the increasing $LW_{\downarrow}$, $TR_{\downarrow}$, T_{2m}, and *SPH*, as well as the weakening WS_{10m}, jointly contribute the LST increase (Shi et al., 2022; Woolway et al., 2019).

4.2. Lake Heatwave

In comparison to long-term lake warming, the anomalous thermal extreme induced by climate change could lead to more severe ecological consequences by altering the thermal/biogeochemical habitats of aquatic species and thus pushing ecosystems to the resilience limits (Kraemer et al., 2021; Woolway, Jennings, et al., 2021), as has already reported during record-breaking atmospheric and marine heatwaves (Laufkötter et al., 2020). Here, we investigate the spatiotemporal variations in the annual mean duration and intensity of LHW over TP (Figure 10).

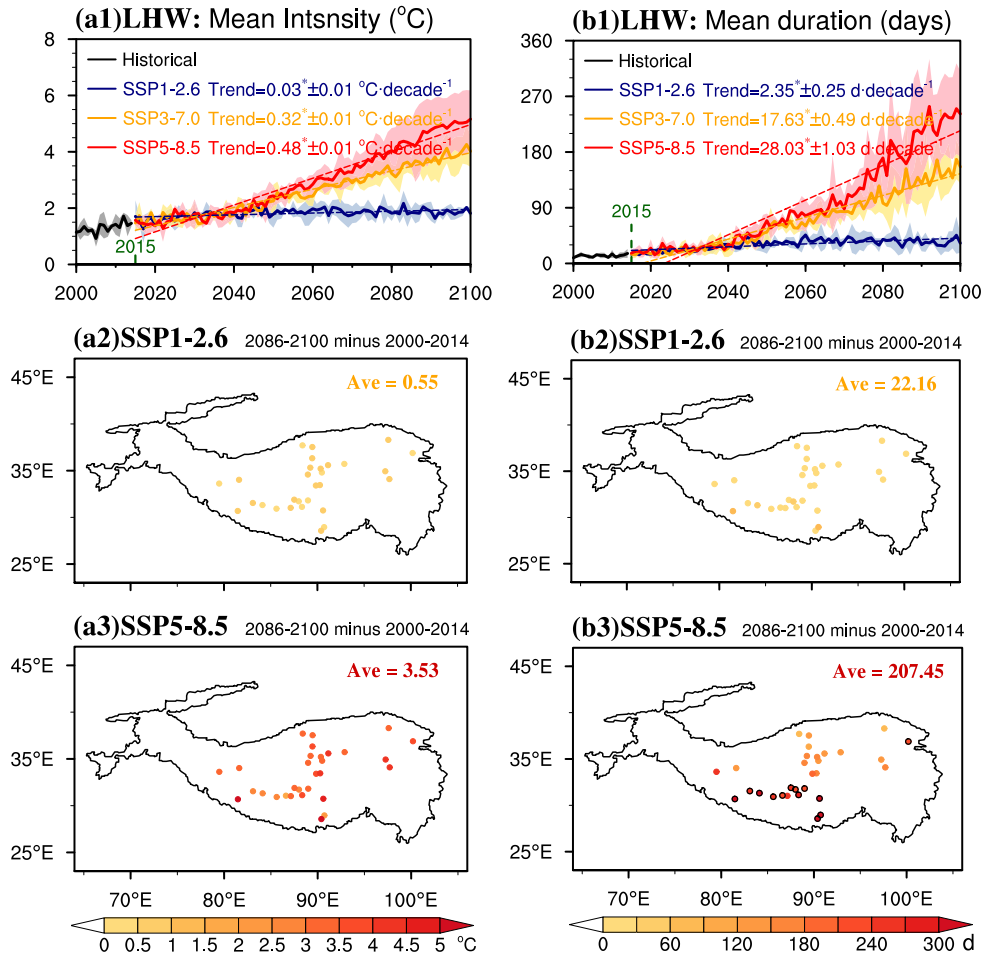

Figure 10. Time series of annual mean (a1) intensity and (b1) duration of lake heatwave (LHW) averaged over all studied lakes during historic (2000–2014) and future (2015–2100) phases, with the formats same as Figure 2. Spatial distributions of the relative change in annual mean (a2), (a3) intensity and (b2), (b3) duration of LHW by the end of twenty-first century (2086–2100 minus 2000–2014) under SSP1-2.6 and SSP5-8.5, with Ave denoting the average across all studied lakes. In (a1) and (b1), the long-term trends are all statistically significant at the 0.05 level and marked with asterisks. In (b3), the black hollow circles denote the lakes projected to reach a permanent LHW state.

During historic phase (2000–2014), a typical LHW event has a mean intensity of 1.31°C and a mean duration of 12.98 days. During future phase (2015–2100), LHW is projected to be more intense and longer-lasting across all studied lakes, with the magnitude of metric changes increasing with the severity of SSP scenarios. Under the most stringent scenario SSP1-2.6, the mean intensity and duration of LHW show a significant upward trend of 0.03 ± 0.01°C·decade^{-1} and 2.35 ± 0.25 d·decade^{-1} (Figures 10a and 10b), and will increase to 1.86°C and 1.7-fold to 35.14 days by the end of this century (2086–2100), respectively. Under the worst scenario SSP5-8.5, the mean intensity and duration of LHW show a significant upward trend of 0.48 ± 0.01°C·decade^{-1} and 28.03 ± 1.03 d·decade^{-1}, and will increase to 4.84°C and 16-fold to 220.43 days during 2086–2100 (Figures 10c and 10d), respectively.

Figure 11 shows the long-term variations in the annual days of four LHW categories during the twenty-first century. During 2000–2014, the moderate category accounts for the majority of LHW events, with an annual mean count of 12.69 days and a percentage contribution of 97.77%. During 2015–2100, LHW days slightly increase and the moderate category is still dominant under SSP1-2.6 (Figure 11a). However, under SSP3-7.0 and SSP5-8.5, LHW occurs more frequently since 2050 and the proportion of strong, severe, and extreme categories increases more rapidly toward the latter stage of this century (Figures 11b and 11c). For example, under SSP5-8.5, the annual mean duration (percentage contribution) of moderate, strong, severe, and extreme LHW during 2086–

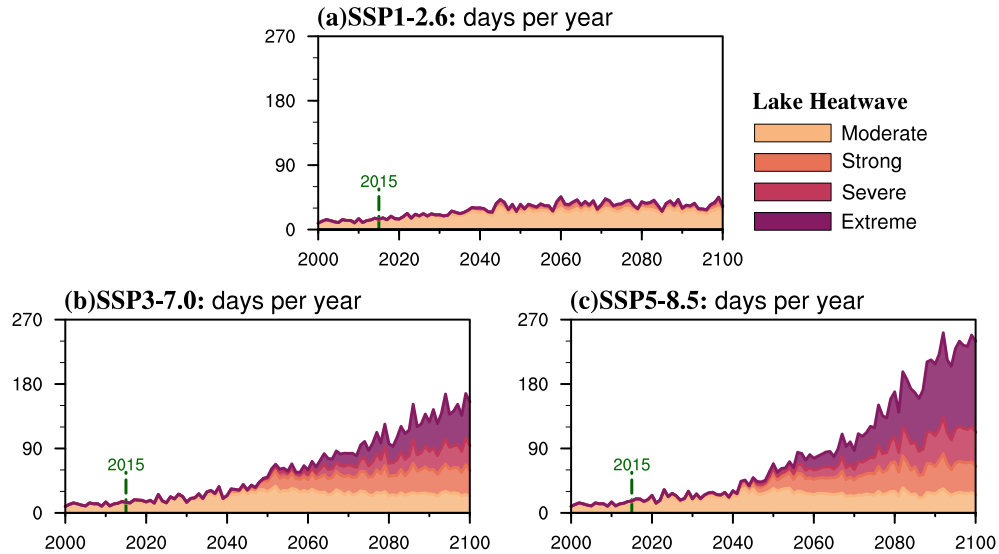

Figure 11. Time series of annual moderate, strong, severe, and extreme LHW days under three SSPs during 2000–2100. All results are based on the average of three GCM-based simulations in 30 studied lakes.

2100 increase to 27.33 days (12.40%), 40.56 days (18.40%), 45.06 days (20.44%), and 107.48 days (48.76%), respectively. The above projections suggest that under medium-high radiative forcing scenarios, what was once considered a short-lived moderate thermal extreme will evolve into a new "normal" thermal state, characterized by longer-lasting and extremely higher temperature spanning multiple seasons. Five (thirteen) of the studied lakes will reach a permanent LHW state under SSP3-7.0 (SSP5-8.5). That is, the projected LST exceeds the 90th percentile threshold continuously over a full year, implying a complete deviation from the present LST climatology.

4.3. Ice and Warm Thermal Stratification

Figures 12 and 13 show the historic and future changes of lake ice and warm thermal stratification, respectively.

During historic phase (2000–2014), lake ice typically forms in early December and persists until early May over TP, with the mean duration and thickness of approximately 164 days and 0.99 m, respectively (Figures 12a1–12a4). The projections suggest a widespread trend toward delayed ice onset, advanced ice break-up, shortened ice duration, and declined ice thickness from 2015 to 2100, with the severity of changes in line with the climate driver shifts. For the low radiative forcing scenario SSP1-2.6 (Figures 12b1–12b4), the ice onset, break-up, duration, and thickness averaged over all studied lakes will become 4.54 days later, 4.78 days earlier, 9.32 days shorter, and 0.06 m thinner by the end of this century (2086–2100). While under SSP5-8.5 (Figures 12c1–12c4), the ice onset, break-up, duration, and thickness have consistent but more pronounced long-term trends of 1.84 ± 0.07 d·decade^{-1}, -2.82 ± 0.10 d·decade^{-1}, -4.66 ± 0.13 d·decade^{-1}, and -0.06 ± 0.00 m·decade^{-1} (significance at the 0.05 level), corresponding to the remarkable end-of-century changes of 24.48 days, −30.07 days, −61.56 days, and −0.43 m. Furthermore, lakes such as NamCo, Tangra Yumco, Yamdrok, Taro Co, Mapam Yumco, and Pumoyong Co are anticipated to permanently lose their ice cover by the end of twenty-first century. These ice phenological changes are highly likely exceeding the ranges of natural variability, and suggest the influence of positive ice-albedo feedback, where the decreased surface albedo due to lake ice retreat acts to cause increased absorption of solar radiation, more pronounced lake warming, and thus reinforce the winter lake ice loss. Subsequently, the earlier break-up of lake ice enables the water to warm more rapidly in early spring via allowing effective radiative heating. This would lead to earlier spring overturning and stratification onset, amplifying the influence of rising downward radiation and air temperature on the lake water temperature during stratified phase, and in turn shift ice phenology toward delayed onset and reduced production. The evidence and cascading effects of ice-albedo feedback have been recognized for both the Arctic Ocean (Kashiwase et al., 2017) and global seasonally ice-covered lakes (Huang et al., 2022; Li et al., 2022), including the Laurentian Great Lakes and Lake Vättern (Austin & Colman, 2007; Weyhenmeyer et al., 2007; Zhong et al., 2016).

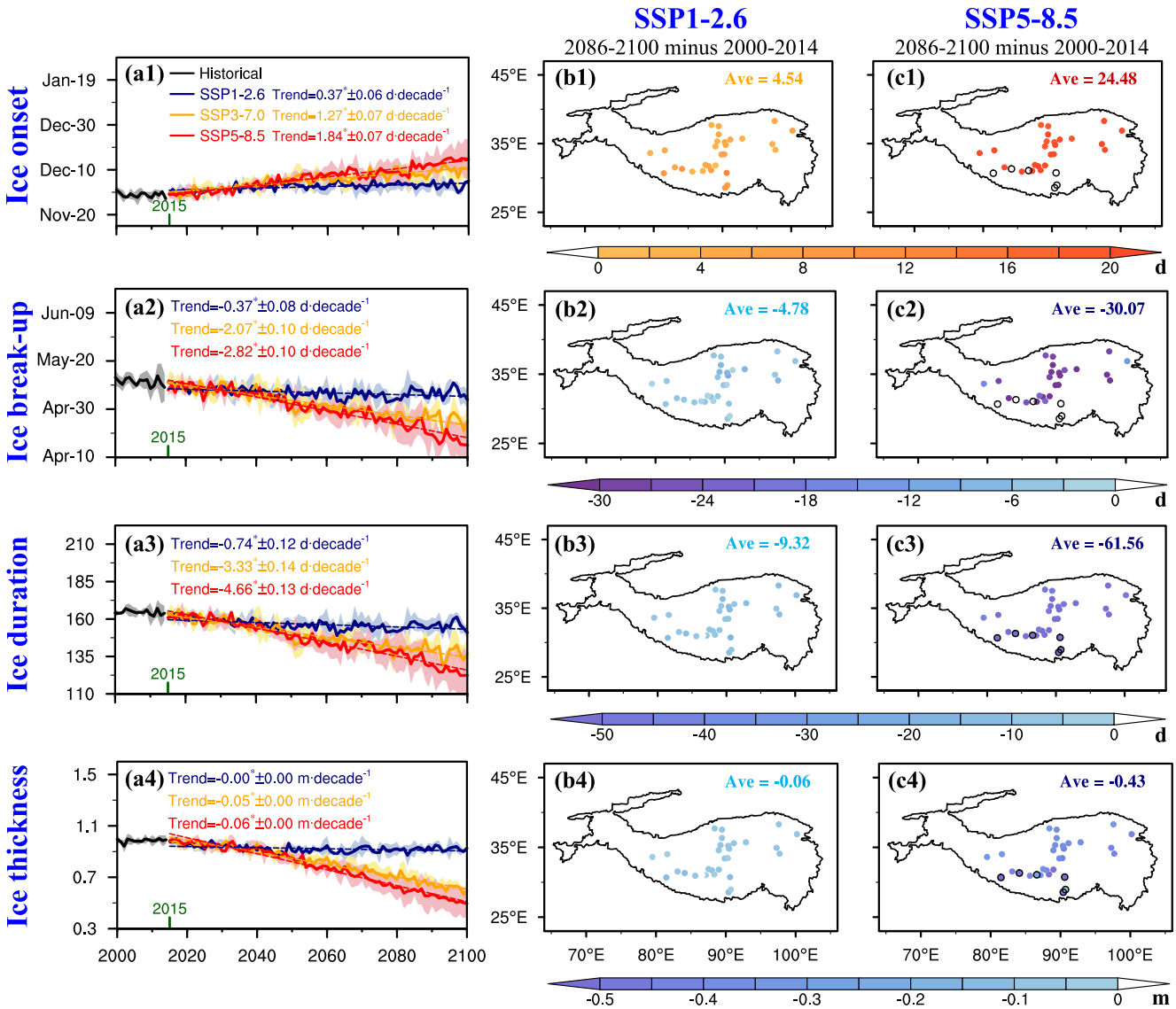

Figure 12. Left column: time series of annual (a1) ice onset, (a2) break-up, (a3) duration, and (a4) thickness averaged over all studied lakes during historic (2000–2014) and future (2015–2100) phases, with the formats same as Figure 2. Middle and right columns: spatial distributions of the relative change in ice onset, break-up, duration, and thickness by the end of twenty-first century (2086–2100 minus 2000–2014) under SSP1-2.6 and SSP5-8.5, respectively. In the left column, the long-term trends are all statistically significant at the 0.05 level and marked with asterisks. In the right two columns, Ave denote the average across all studied lakes, and the black circles denote the lakes projected to permanently lose ice cover.

During historic phase (2000–2014), lake thermal stratification typically begins in early June and persists until late October, with a duration of 143 days (Figures 13a1–13a3). In the projected future phase (2015–2100), the increasing $TR_{\downarrow}$ and T_{2m} cause intensified heating, and the decreasing WS_{10m} cause weakened turbulent heat loss and vertical mixing. The combined effects are anticipated to result in an earlier onset, later break-up, and prolonged duration in stratification, with the severity of changes in line with the shifts in climate drivers. The stratification onset, break-up, and duration averaged across all studied lakes are projected to undergo the modest end-of-century changes during most stringent emission scenario SSP1-2.6, with respective values of −7.10, 4.08, and 11.18 days (Figures 13b1–13b3). While under the high emission scenario SSP5-8.5 (Figures 13c1–13c3), the projected long-term trends for stratification onset, break-up, and duration are much larger at -6.27 ± 0.14, 2.24 ± 0.05, and 8.51 ± 0.16 d·decade^{-1} (significance at the 0.05 level), corresponding to the remarkable end-of-century changes of −46.83, 18.62, and 65.46 days. It is noteworthy that the advancing stratification onset shows evidently more pronounced trends and relative changes than the delaying stratification break-up. This can be

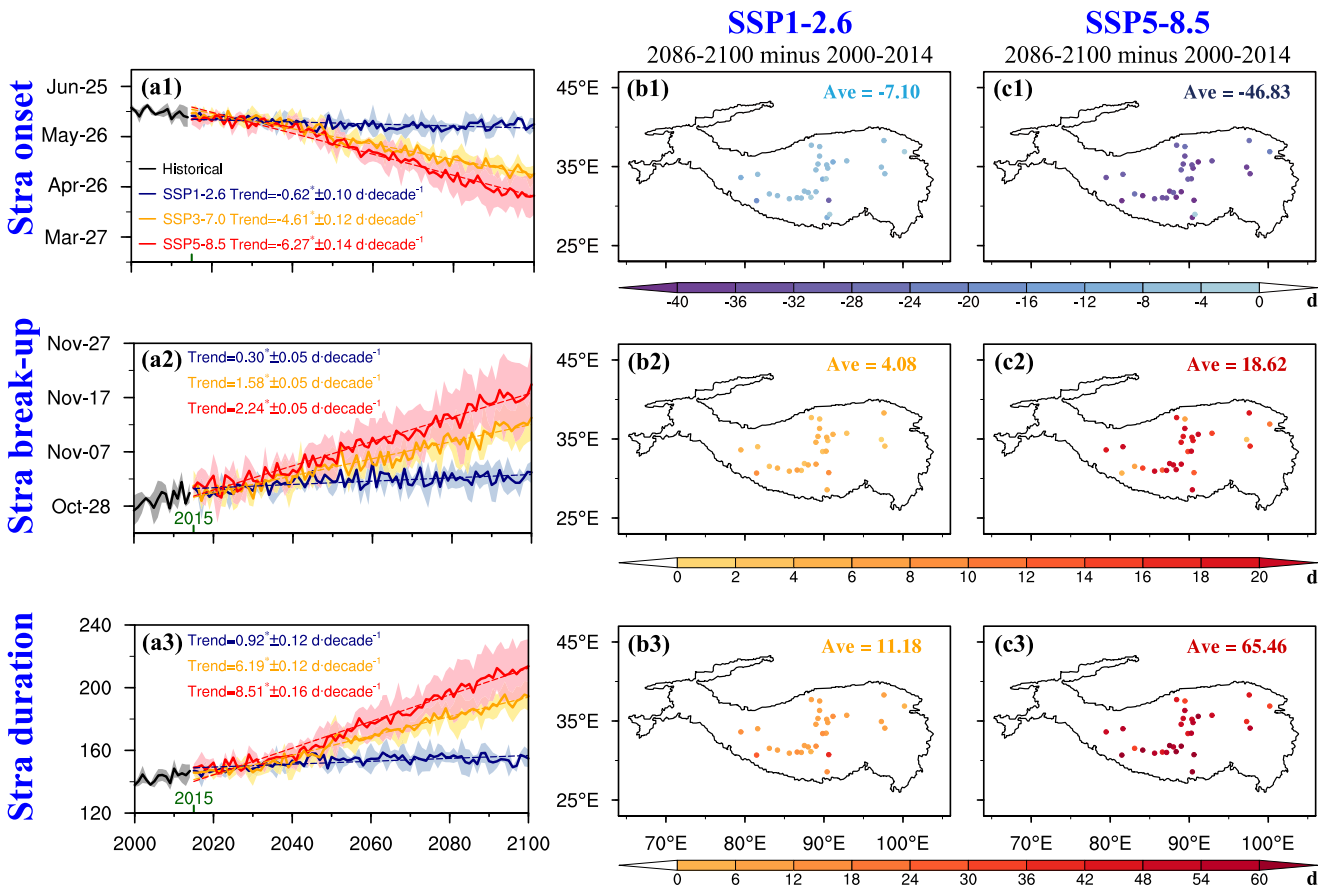

Figure 13. Same as Figure 12, but for warm thermal stratification onset, break-up, and duration. In (a1)–(a3), "Stra" is the abbreviation of "Stratification".

explained by the strong linear relationship between earlier ice break-up and stratification onset, as also highlighted in a phenological study on Northern Hemisphere lakes by Woolway, Sharma, et al. (2021).

4.4. Mixing Regime

Lake mixing regime depends on whether it experiences ice cover and the annual counts of continuous vertical mixing phase (Lewis, 1983). At present, the majority of large seasonally ice-covered lakes are categorized as dimictic (meaning they experience two annual mixing phases), with few exceptions such as Dogze Co, which is a meromictic lake that experiences incomplete mixing due to the existence of monimolimnion related to high salinity gradient (Wang et al., 2014). In future scenarios, the climate-related changes in LST, ice, and stratification are expected to qualitatively modify the lake mixing regime. To address this, Figure 14 shows the historic and future daily evolution of lake ice and water temperature profile in Lake Mapam Yumco. From Figure 14a, Lake Mapam Yumco is a typical dimictic lake over TP, featured by long-lasting inversely stratified and stratified phases during winter and summer, and two following complete overturning mixing phases in spring and autumn. However, as the influence of anthropogenic radiative forcing intensifies in the future (Figures 14a–14c), the lake will experience substantial winter ice loss, accelerated ice melt, and earlier establishment of summer thermal stratification. The mixed layer temperature during stratified phase is projected to significantly increase, acting in conjunction with the decreased WS_{10m} to cause an anomalously stable and persistent stratification, further delaying the ice onset. In the extreme SSP5-8.5 scenario, lake water temperature remains above *Tdmax* (Figure 14d), estimated to be 3.93°C with a pressure of 0.57 bar and a salinity of 0.2 g L^{-1} for Lake Mapam Yumco, since the break-up of stratification. The lake no longer freezes during winter, and instead of forming the historic inverse stratification, it stays in a thermally mixed state until thermal stratification onset in the following year. This indicates a shift in the lake's mixing regime from dimictic to warm monomictic.

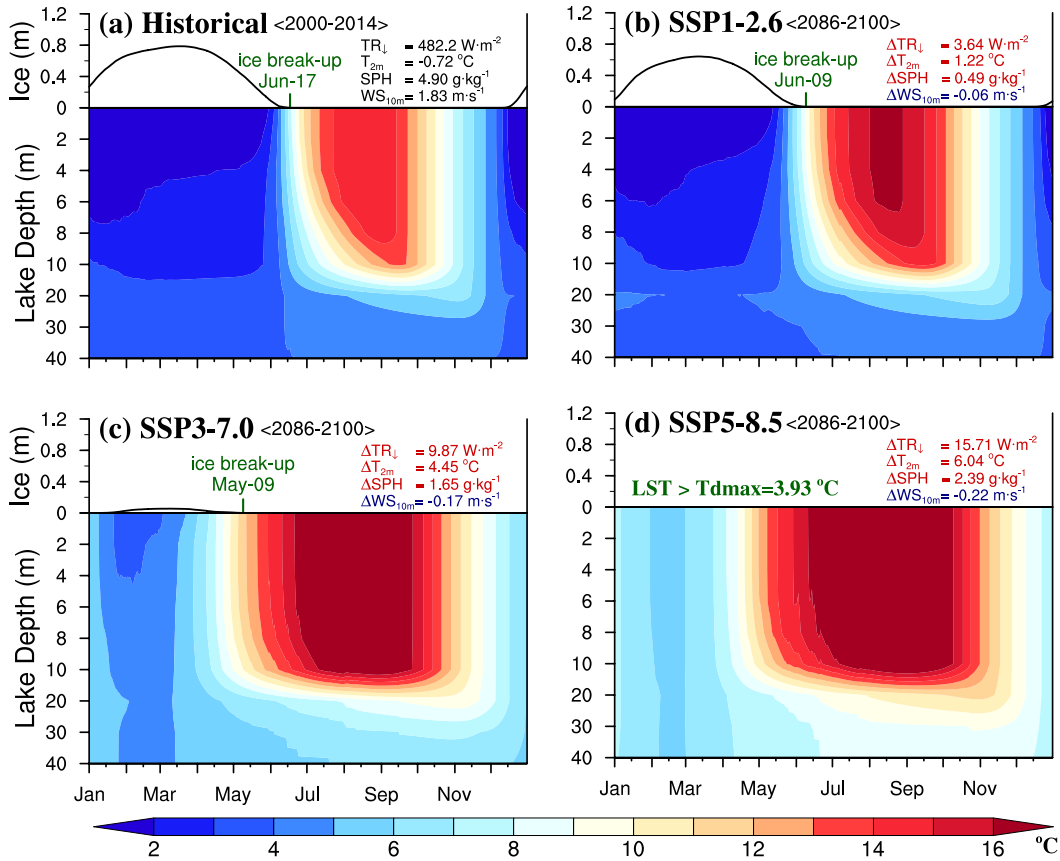

Figure 14. Daily evolution of ice thickness and water temperature profile in Lake Mapam Yumco (a) during 2000–2014 and during 2086–2100 under (b) SSP1-2.6, (c) SSP3-7.0, and (d) SSP5-8.5. All results are based on the ensemble mean simulations under three GCM-based forcings. In (a), texts in black denote the annual mean $TR_{\downarrow}$, T_{2m}, SPH, and WS_{10m} during 2000–2014, and in (b)–(d), texts in red and blue denote their end-of-century changes (2086–2100 minus 2000–2014).

5. Summary, Discussion and Future Recommendations

In this study, we use the 1-D offline WRF-Lake model to assess the influence of climate change on large-lake thermodynamics over TP. The model was driven by the atmospheric forcing variables from three bias-corrected GCM projections of twenty-first-century climate under three SSPs. The validation during historic phase (2000–2014) shows that the model can reasonably reproduce the seasonality and magnitude of LST relative to MODIS observations, with a mean TC of 0.88 and BIAS of 0.48°C averaged across all studied lakes.

From 2015 to 2100, large lake basins are projected to experience consistent increases in $LW_{\downarrow}$, $TR_{\downarrow}$, T_{2m}, SPH, along with decreases in $SW_{\downarrow}$, and WS_{10m}. The combined impacts of climate changes correspond to widespread lake warming, declined ice cover, shortened ice duration, and prolonged warm thermal stratification. These changes are more pronounced with the severity of anthropogenic climate shifts. Under the worst scenario SSP5-8.5, the trends of annual LST, ice thickness, ice duration, and stratification duration averaged across all studied lakes are 0.65 ± 0.01°C·decade^{-1}, −0.06 ± 0.00 m·decade^{-1}, -4.66 ± 0.13 d·decade^{-1}, 8.51 ± 0.16 d·decade^{-1}, and LHW will become hotter (0.48 ± 0.01°C·decade^{-1}) and longer (28.03 ± 1.03 d·decade^{-1}). Note that the positive ice-albedo feedback is likely to exacerbate the influence of climate changes by accelerating the ice break-up (−2.82 ± 0.10 d·decade^{-1}) and stratification onset (−6.27 ± 0.14 d·decade^{-1}), which in turn contributes to the stronger lake warming during winter and summer months. By the end of this century, the extreme heatwaves are anticipated to occur more frequently and across multiple seasons, and nearly half of the studied lakes will reach a permanent heatwave state. With the lake temperature irreversibly moving out of its natural variability, those lakes featured by significant warming are found to intermittently or permanently lose seasonal ice cover and tend to exhibit anomalous mixing regimes. In the extreme case, the common alteration in lake mixing regimes over TP is from dimitic to warm monomictic, implying remarkably weakened vertical mixing strength. Nonetheless, by

adhering to the most stringent scenario SSP1-2.6, rapid lake warming, accelerated ice loss, frequent occurrence of extreme LHW, and potential shifts in mixing regimes can be avoided.

There is compelling observational evidence that the lake warming (Carrea et al., 2019; O'Reilly et al., 2015), phenological shifts in ice and stratification (Fichot et al., 2019; Kraemer et al., 2015; Sharma & Woolway, 2021), and mixing regime alterations (Anderson et al., 2021; Ficker et al., 2017; Woolway & Merchant, 2019) are already under way, and exert widespread influences on the lake physical and chemical processes. We expect that the projected out-of-control climate-related lake thermal changes will cause numerous and adverse biogeochemical consequences. First is the anticipated increase of evaporative rates due to the warming surface waters during prolonged open-water phase. Globally, annual mean lake evaporation is expected to increase by 16% from 2006 to 2015 to 2091–2100 under the high-emission RCP8.5 scenario (Wang et al., 2018). On one hand, the enhanced evaporative water loss plays a critical role in lake water balances (Zhao et al., 2022), with negative implications for the rapid TP lake expansion induced by the increasing precipitation and terrestrial runoff. On the other hand, the resulting intensified turbulent heat and water flux may pose feedback to the regional lake-effect clouds and precipitation (Rüthrich et al., 2015; Yao et al., 2023). A notable example is the projected intensification of hazardous thunderstorms over Lake Victoria under high-emission scenarios (Thiery et al., 2016). Thus, it is imperative to further address the future variations in lake evaporation and the cascading impacts over TP. Second, the stronger and longer-lasting stratification couples to less frequently vertical exchange of nutrients and dissolved gases. The impact on oxygen exchanges can work together with the temperature-induced decrease of oxygen solubility to result in lake deoxygenation and ecological productivity decline (Pilla & Williamson, 2021; Steinsberger et al., 2020). The release of methane, phosphorus, toxic metal ions due to mineralization or anaerobic processes (Borges et al., 2015; Hupfer & Lewandowski, 2008), as well as the occurrence of harmful algal blooms (Brookes & Carey, 2011), may be amplified, posing serious threats to the lake water quality and habitats of aquatic organisms (Till et al., 2019; Zhang et al., 2015). In the future, understanding the ongoing cascading ecological influence of thermal changes is also an urgent task to identify equilibrium points and determine management strategies for sustaining the lake biodiversity and ecosystem functioning over TP.

Although the modeled lake thermal variations exhibit good consistency across three GCM-based simulations, we must admit that adopting an ensemble framework with broader ranges of atmospheric forcings and physically based lake models is essential for advancing a more comprehensive and convincing understanding of present results. Moreover, several study limitations should be carefully considered to better predict and understand the projected lake thermal response to climate change. First, the influence of glacier and snow cover changes on lake thermodynamics is not resolved by the model but important for these high-altitude lakes. For example, despite the overall warming trend of LST over TP during the past two decades, a cooling trend is detected for the glacier-fed lakes located at elevations above 4,200 m (Song et al., 2016; Wan et al., 2018; Zhang et al., 2014), leading to a higher mean warming rate in non-glacier-fed lakes compared to glacier-fed ones (Zhang et al., 2020). This phenomenon is linked to the accelerated cold-water supply from the observed rapid melting of glaciers and perennial snow cover (Bolch, 2012; Yao et al., 2019, 2022; Zhang et al., 2023). In our research, 26 of the studied lakes are discharged by the glacier-melt/snow-melt runoff (Guo et al., 2021). We expect the projected lake warming to be overestimated since the negative effect of cryospheric degradation will be likely amplified under a warming climate over TP. Neglecting the change of over-lake snow cover can introduce additional uncertainties into the projections. Specifically, the presence of snowpack and snow ice, acting as a reflective and insulating layer due to their high albedo and low thermal conductivity (Adam, 1976; Sturm et al., 1997), results in the accumulation of thicker lake ice toward the end of ice season, followed by rapid melting (Brown & Duguay, 2010, 2011). Less snow cover corresponds to earlier ice break-up by augmenting the available amount of solar radiation absorbed for melting (Vavrus et al., 1996; Woolway et al., 2020), thus advancing the onset of spring overturning and thermal stratification. Considering the significant air warming over TP has led to the decrease of snowfall/rainfall ratio over the past half century (Wang et al., 2016), a trend also noted in future projections (Nury et al., 2022), it is imperative to further investigate the influence of this factor on lake thermal projections. Second, we must admit that the utilized offline (one-way driven) simulation cannot fully capture the dynamic lake-atmosphere feedback mechanisms involved in online lake-atmosphere coupled simulations, such as the modification of local microclimate (temperature, humidity, and wind) by lake surface temperature and turbulent fluxes, which could, in turn, influence the lake thermodynamics and mixing processes. The missing representation of these dynamic lake-atmosphere feedbacks in offline simulations generally adds the projection uncertainty of lake thermal response to future climate change. Third, the interannual variability of lake ice phenology, which is significantly influenced by

weather-climate anomalies and large-scale teleconnection patterns, for example, the El Niño-Southern Oscillation, Arctic Oscillation, and North Atlantic Oscillation (Bai et al., 2012; Fujisaki et al., 2013; Imrit & Sharma, 2021), is not accurately captured by the offline WRF-Lake. The model's poor predictability primarily arises from lake ice phenology's highly sensitive and nonlinear response to the complex variability of climate forcings (Benson et al., 2012; Richardson et al., 2024). This issue is underscored by Wang et al. (2012), who, using satellite observations of the Laurentian Great Lakes from 1973 to 2010, observed that the standard deviations in annual ice cover were comparable or sometimes even larger than the climatological means for all five lakes. Additionally, the limited predictive capability of natural climate variability in GCM climate forcings, combined with the lake model's insufficient representation of ice-related processes, further contributes to the challenge in accurately simulating the interannual variability of lake ice phenology. Fourth, in marine/lake heat wave definitions (Hobday et al., 2016), a period of 30 years, which is almost the full period of recorded satellite sea surface temperature observations, is recommended to define a baseline temperature climatology. A sufficiently long baseline whenever possible is also emphasized by previous applications, for example, 1982–2005 by Oliver et al. (2017) and 1970–1999 by Woolway, Jennings, et al. (2021). Hence, when interpreting the LHW shown in Section 4.2, one should bear in mind that a 15-year baseline, covering the historic phase of 2000–2014, may not effectively capture the long-time scales of LST variability. Finally, to what extent the lake thermodynamics are altered by individual atmospheric forcing variables deserves further quantitative attribution analysis.

Data Availability Statement

The integrated dataset of daily lake surface temperature for 160 lakes over TP can be downloaded from https://doi.org/10.5281/zenodo.5111400 (Guo et al., 2021). The lake ice phenology dataset of 132 lakes across TP from 1978 to 2016 is available on https://figshare.com/articles/dataset/TPLIP/18852338 (Wu et al., 2022). The field observed lake water quality parameters of 124 closed lakes over TP (Zhu, 2021) are available on the National Tibetan Plateau Data Center (https://data.tpdc.ac.cn/en/). The bias-corrected GFDL-ESM4, IPSL-CM6A-LR and MPI-ESM1-2-HR projections from ISIMIP3b are available on https://www.isimip.org/protocol/3/ (Lange & Büchner, 2021). We acknowledge the use of Python Package "marineHeatWaves" (http://github.com/ecjoliver/marineHeatWaves) to detect lake heatwaves, and the NCAR Command Language version 6.6.2 (http://dx.doi.org/10.5065/D6WD3XH5) to analyze model results and plot all the figures.

Acknowledgments
This study is funded by the National Natural Science Foundation of China under Grants 41975081, 42305015, Natural Science Foundation of Tibet Autonomous Region (Grant XZ202201ZR0046G), the Beijige Open Research Fund under Grant BJG202403, CAS "Light of West China" Program (E129030101), the basic research fund of CAMS (2023Y012), the research project of Jiangsu Meteorological Bureau (KQ202313), Science and Technology Commission of Shanghai Municipality, Morning Star Project Sailing Program (23YF1440100), the Research Funds for the Frontiers Science Center for Critical Earth Material Cycling Nanjing University, the Fundamental Research Funds for the Central Universities (020914380103), the Jiangsu University "Blue Project" outstanding young teachers training object, the Jiangsu Collaborative Innovation Center for Climate Change, National Key Research and Development Program of China under Grant 2022YFC3080500.

References

Adams, W. P. (1976). Diversity of lake cover and its implications. *Musk-Ox*, *181*, 86–98.
Adrian, R., O'Reilly, C. M., Zagarese, H., Baines, S. B., Hessen, D. O., Keller, W., et al. (2009). Lakes as sentinels of climate change. *Limnology & Oceanography*, *54*(6), 2283–2297. https://doi.org/10.4319/lo.2009.54.6_part_2.2283
Anderson, E. J., Stow, C. A., Gronewold, A. D., Mason, L. A., McCormick, M. J., Qian, S. S., et al. (2021). Seasonal overturn and stratification changes drive deep-water warming in one of Earth's largest lakes. *Nature Communications*, *12*(1), 1688. https://doi.org/10.1038/s41467-021-21971-1
Austin, J. A., & Colman, S. M. (2007). Lake superior summer water temperatures are increasing more rapidly than regional air temperatures: A positive ice-albedo feedback. *Geophysical Research Letters*, *34*(6). https://doi.org/10.1029/2006GL029021
Bai, X. Z., Wang, J., Sellinger, C., Clites, A., & Assel, R. (2012). Interannual variability of Great Lakes ice cover and its relationship to NAO and ENSO. *Journal of Geophysical Research*, *117*(C3). https://doi.org/10.1029/2010JC006932
Benson, B. J., Magnuson, J. J., Jensen, O. P., Card, O. P., Hodgkins, G., Korhonen, J., et al. (2012). Extreme events, trends, and variability in Northern Hemisphere lake-ice phenology (1855-2005). *Climatic Change*, *112*(2), 299–323. https://doi.org/10.1007/s10584-011-0212-8
Bolch, T., Kulkarni, A., Kääb, A., Huggel, C., Paul, F., Cogley, J. G., et al. (2012). The state and fate of Himalayan glaciers,. *Science*, *336*(6079), 310–314. https://doi.org/10.1126/science.1215828
Borges, A. V., Darchambeau, F., Teodoru, C. R., Marwick, T. R., Tamooh, F., Geeraert, N., et al. (2015). Globally significant greenhouse-gas emissions from African inland waters. *Nature Geoscience*, *8*, 637–642. https://doi.org/10.1038/ngeo2486
Brookes, J. D., & Carey, C. C. (2011). Resilience to blooms. *Science*, *334*(6052), 46–47. https://doi.org/10.1126/science.1207349
Brown, L. C., & Duguay, C. R. (2010). The response and role of ice cover in lake-climate interactions. *Progress in Physical Geography*, *34*(5), 671–704. https://doi.org/10.1177/0309133310375653
Brown, L. C., & Duguay, C. R. (2011). A comparison of simulated and measured lake ice thickness using a Shallow Water Ice Profiler. *Hydrological Processes*, *25*(19), 2932–2941. https://doi.org/10.1002/hyp.8087
Brownlee, K. A. (1965). *Statistical theory and methodology in science and engineering*. John Wiley and Sons.
Bukata, R. P., Jerome, J. H., & Bruton, J. E. (1988). Relationships among Secchi disk depth, beam attenuation coefficient, and irradiance attenuation coefficient for great-lakes waters. *Journal of Great Lakes Research*, *14*(3), 347–355. https://doi.org/10.1016/S0380-1330(88)71564-6
Cai, Y., Ke, C. Q., Li, X. G., Zhang, G. Q., Duan, Z., & Lee, H. (2019). Variations of lake ice phenology on the Tibetan Plateau from 2001 to 2017 based on MODIS data. *Journal of Geophysical Research*, *124*(2), 825–843. https://doi.org/10.1029/2018JD028993
Cai, Y., Ke, C. Q., Xiao, Y., & Wu, J. (2022). What caused the spatial heterogeneity of lake ice phenology changes on the Tibetan Plateau? *The Science of the Total Environment*, *836*, 155517. https://doi.org/10.1016/j.scitotenv.2022.155517

Carrea, L., Woolway, I. R., Merchant, C. J., Dokulil, M. T., DeGasperi, C., Eyto, E. D., et al. (2019). Lake surface water temperature [in "State of the Climate in 2019"]. *Bulletin of the American Meteorological Society*, *101*, S26–S28. https://doi.org/10.1175/2020BAMSStateoftheClimate.1

Chen, C. T. A., & Millero, F. J. (1986). Thermodynamic properties for natural waters covering only the limnological range. *Limnology & Oceanography*, *31*(3), 657–662. https://doi.org/10.4319/lo.1986.31.3.0657

Chen, D. L., Xu, B. Q., Yao, T. D., Guo, Z. T., Cui, P., Chen, F. H., et al. (2015). Assessment of past, present and future environmental changes on the Tibetan Plateau (in Chinese). *Chinese Science Bulletin*, *60*(32), 3025–3303. https://doi.org/10.1360/N972014-01370

Chen, J. M., & Liao, J. J. (2020). Monitoring lake level changes in China using multi-altimeter data (2016-2019). *Journal of Hydrology*, *590*, 125544. https://doi.org/10.1016/j.jhydrol.2020.125544

Davison, W. (1981). Supply of iron and manganese to an anoxic lake basin. *Nature*, *290*(5803), 241–243. https://doi.org/10.1038/290241a0

Feng, L., Dai, Y. H., Hou, X. J., Xu, Y., Liu, J. G., & Zheng, C. M. (2021). Concerns about phytoplankton bloom trends in global lakes. *Nature*, *590*(7846), E35–E47. https://doi.org/10.1038/s41586-021-03254-3

Fichot, C. G., Matsumoto, K., Holt, B., Gierach, M. M., & Tokos, K. S. (2019). Assessing change in the overturning behavior of the Laurentian Great Lakes using remotely sensed lake surface water temperatures. *Remote Sensing of Environment*, *235*, 111427. https://doi.org/10.1016/j.rse.2019.111427

Ficker, H., Luger, M., & Gassner, H. (2017). From dimictic to monomictic: Empirical evidence of thermal regime transitions in three deep alpine lakes in Austria induced by climate change. *Freshwater Biology*, *62*(8), 1–11. https://doi.org/10.1111/fwb.12946

Fujisaki, A., Wang, J., Bai, X. Z., Leshkevich, G., & Lofgren, B. (2013). Model-simulated interannual variability of Lake Erie ice cover, circulation, and thermal structure in response to atmospheric forcing, 2003-2012. *Journal of Geophysical Research*, *118*(9), 4286–4304. https://doi.org/10.1002/jgrc.20312

Grant, L., Vanderkelen, I., Gudmundsson, L., Tan, Z. L., Perroud, M., Stepanenko, V. M., et al. (2021). Attribution of global lake systems change to anthropogenic forcing. *Nature Geoscience*, *14*(11), 849–854. https://doi.org/10.1038/s41561-021-00833-x

Gu, H. P., Jin, J. M., Wu, Y. H., Ek, M. B., & Subin, Z. M. (2015). Calibration and validation of lake surface temperature simulations with the coupled WRF-lake model. *Climatic Change*, *129*(3–4), 471–483. https://doi.org/10.1007/s10584-013-0978-y

Guo, L. N., Wu, Y. H., Zheng, H. X., Zhang, B., Li, J. S., Zhang, F. S., & Shen, Q. (2018). Uncertainty and variation of remotely sensed lake ice phenology across the Tibetan Plateau. *Remote Sensing*, *10*, 1534. https://doi.org/10.3390/rs10101534

Guo, L. N., Zheng, H. X., Wu, Y. H., Fan, L. X., Wen, M. X., Li, J. S., et al. (2021). An integrated dataset of daily lake surface temperature over Tibetan Plateau. [Dataset]. *Earth System Science Data*, *14*(7), 3411–3422. https://doi.org/10.5194/essd-2021-151

Henderson-Sellers, B. (1985). New formulation of eddy diffusion thermocline models. *Applied Mathematical Modelling*, *9*(6), 441–446. https://doi.org/10.1016/0307-904X(85)90110-6

Henderson-Sellers, B., & Davies, A. M. (1989). Thermal stratification modeling for oceans and lakes. *Annual Review of Heat Transfer*, *2*, 86–156. https://doi.org/10.1615/AnnualRevHeatTransfer.v2.50

Ho, J. C., Michalak, A. M., & Pahlevan, N. (2019). Widespread global increase in intense lake phytoplankton blooms since the 1980s. *Nature Climate Change*, *574*(7780), 667–670. https://doi.org/10.1038/s41586-019-1648-7

Hobday, A. J., Alexander, L. V., Perkins, S. E., Smale, D. A., Straub, S. C., Oliver, E. C. J., et al. (2016). A hierarchical approach to defining marine heatwaves. *Progress in Oceanography*, *141*, 227–238. https://doi.org/10.1016/j.pocean.2015.12.014

Hobday, A. J., Oliver, E. C. J., Gupta, A. S., Benthuysen, J. A., Burrows, M. T., Donat, M. G., et al. (2018). Categorizing and naming marine heatwaves. *Oceanography*, *31*(2), 162–173. https://doi.org/10.5670/oceanog.2018.205

Hook, S. J., Prata, J., Alley, R. E., Abtahi, A., Richards, R. C., Schladow, S. G., & Pálmarsson, G. (2003). Retrieval of lake bulk and skin temperature using Along-Track Scanning Radiometer (ATSR-2) data: A case study using Lake Tahoe, California. *Journal of Atmospheric and Oceanic Technology*, *20*(4), 534–548. https://doi.org/10.1175/1520-0426(2003)20<534:ROLBAS>2.0.CO;2

Hostetler, S. W., & Bartlein, P. J. (1990). Simulation of lake evaporation with application to modeling lake level variations of Harney-Malheur Lake. *Oregon. Water Resour. Res.*, *26*(10), 2603–2612. https://doi.org/10.1029/WR026i010p02603

Huang, A. N., Lazhu, Wang, J. B., Dai, Y. J., Yang, K., Wei, N., et al. (2019). Evaluating and improving the performance of three 1-D lake models in a large deep lake of the Central Tibetan Plateau. *Journal of Geophysical Research*, *124*(6), 3143–3167. https://doi.org/10.1029/2018JD029610

Huang, L., Timmermann, A., Lee, S. S., Rodgers, K. B., Yamaguchi, R., & Chung, E. S. (2022). Emerging unprecedented lake ice loss in climate change projections. *Nature Communications*, *13*(1), 5798. https://doi.org/10.1038/s41467-022-33495-3

Huang, L., Wang, J. B., Zhu, L. P., Ju, J. T., & Daut, G. (2017). The warming of large lakes on the Tibetan Plateau: Evidence from a lake model simulation of Nam Co, China, during 1979-2012. *Journal of Geophysical Research*, *122*(13), 95–107. https://doi.org/10.1002/2017JD027379

Huang, L., Wang, X. H., Sang, Y. X., Tang, S. C., Jin, L., Yang, H., et al. (2021). Optimizing lake surface water temperature simulations over large lakes in China with FLake model. *Earth and Space Science*, *8*. https://doi.org/10.1029/2021EA001737

Hupfer, M., & Lewandowski, J. (2008). Oxygen controls the phosphorus release from lake sediments-a long-lasting paradigm in limnology. *International Review of Hydrobiology*, *93*(4–5), 415–432. https://doi.org/10.1002/iroh.200711054

Imrit, M. A., & Sharma, S. (2021). Climate change is contributing to faster rates of lake ice loss in lakes around the Northern Hemisphere. *Journal of Geophysical Research*, *126*(7). https://doi.org/10.1029/2020JG006134

Jane, S. F., Hansen, G. J. A., Kraemer, B. M., Leavitt, P. R., Mincer, J. L., North, R. L., et al. (2021). Widespread deoxygenation of temperate lakes. *Nature*, *594*(7861), 66–70. https://doi.org/10.1038/s41586-021-03550-y

Kashiwase, H., Ohshima, K. I., Nihashi, S., & Eicken, H. (2017). Evidence for ice-ocean albedo feedback in the Arctic Ocean shifting to a seasonal ice zone. *Scientific Reports*, *7*(1), 8170. https://doi.org/10.1038/s41598-017-08467-z

Ke, L. H., & Song, C. Q. (2014). Remotely sensed surface temperature variation of an inland saline lake over the central Qinghai-Tibet Plateau. *ISPRS J. Photogramm.*, *98*, 157–167. https://doi.org/10.1016/j.isprsjprs.2014.09.007

Kirillin, G., Wen, L. J., & Shatwell, T. (2017). Seasonal thermal regime and climatic trends in lakes of the Tibetan highlands. *Hydrology and Earth System Sciences*, *21*(4), 1895–1909. https://doi.org/10.5194/hess-21-1895-2017

Kraemer, B. M., Anneville, D., Chandra, S., Dix, M., Kuusisto, E., Livingstone, D. M., et al. (2015). Morphometry and average temperature affect lake stratification responses to climate change. *Geophysical Research Letters*, *42*(12), 4981–4988. https://doi.org/10.1002/2015GL064097

Kraemer, B. M., Pilla, R. M., Woolway, R. I., Anneville, O., Ban, S., Montero, W. C., et al. (2021). Climate change drives widespread shifts in lake thermal habitat. *Nature Climate Change*, *11*(6), 521–529. https://doi.org/10.1038/s41558-021-01060-3

Kuang, X. X., & Jiao, J. J. (2017). Review on climate change on the Tibetan Plateau during the last half century. *Journal of Geophysical Research*, *121*(8), 3979–4007. https://doi.org/10.1002/2015JD024728

Lange, S., & Büchner, B. (2021). ISIMIP3b bias-adjusted atmospheric climate input data (v1.1). ISIMIP Repository. [Dataset]. https://doi.org/10.48364/ISIMIP.842396.1

Laufkötter, C., Zscheischler, J., & Frölicher, T. L. (2020). High-impact marine heatwaves attributable to human-induced global warming. *Science*, *369*(6511), 1621–1625. https://doi.org/10.1126/science.aba0690

Layden, A., MacCallum, S. N., & Merchant, C. J. (2016). Determining lake surface water temperatures worldwide using a tuned one-dimensional lake model (FLake, v1). *Geoscientific Model Development*, *9*(6), 2167–2189. https://doi.org/10.5194/gmd-9-2167-2016

Layden, A., Merchant, C., & MacCallum, S. (2015). Global climatology of surface water temperatures of large lakes by remote sensing. *International Journal of Climatology*, *35*(15), 4464–4479. https://doi.org/10.1002/joc.4299

Lei, Y. B., Yao, T. D., Yang, K., Ma, Y., Ma, Y. M., & Bird, B. W. (2021). Contrasting hydrological and thermal intensities determine seasonal lake-level variations - A case study at Paiku Co on the southern Tibetan Plateau. *Hydrology and Earth System Sciences*, *25*(6), 3163–3177. https://doi.org/10.5194/hess-25-3163-2021

Lewis, W. M., Jr. (1983). A revised classification of lakes based on mixing. *Canadian Journal of Fisheries and Aquatic Sciences*, *40*(10), 1779–1787. https://doi.org/10.1139/f83-207

Li, L. L., & Xue, B. (2021). Methane emissions from northern lakes under climate change: A review. *SN Applied Sciences*, *3*(12), 883. https://doi.org/10.1007/s42452-021-04869-x

Li, X. Y., Peng, S. S., Xi, Y., Woolway, R. I., & Liu, G. (2022). Earlier ice loss accelerates lake warming in the Northern Hemisphere. *Nature Communications*, *13*(1), 5156. https://doi.org/10.1038/s41467-022-32830-y

Liu, B. J., Wan, W., Xie, H. J., Li, H., Zhu, S. Y., Zhang, G. Q., et al. (2019). A long-term dataset of lake surface water temperature over the Tibetan Plateau derived from AVHRR 1981-2015. *Scientific Data*, *6*(1), 48. https://doi.org/10.1038/s41597-019-0040-7

Ma, X. G., Yang, K., La, Z., Lu, H., Jiang, Y. Z., Zhou, X., et al. (2022). Importance of parameterizing lake surface and internal thermal processes in WRF for simulating freeze onset of an alpine deep lake. *Journal of Geophysical Research*, *127*(18). https://doi.org/10.1029/2022JD036759

Maberly, S. C., O'Donnell, R. A., Woolway, R. I., Cutler, M. E. J., Gong, M. Y., Jones, I. D., et al. (2020). Global lake thermal regions shift under climate change. *Nature Communications*, *11*(1), 1232. https://doi.org/10.1038/s41467-020-15108-z

Merz, E., Saberski, E., Gilarranz, L. J., Isles, P. D. F., Sugihara, G., Berger, C., & Pomati, F. (2023). Disruption of ecological networks in lakes by climate change and nutrient fluctuations. *Nature Climate Change*, *13*(4), 389–396. https://doi.org/10.1038/s41558-023-01615-6

Millero, F. J. (1978). Freezing point of seawater. Annex 6, Eight report of the joint panel on oceanographic tables and standards (JPOTS). *UNESCO Technical Papers in Marine Science*, *28*.

Niedrist, G. H., Psenner, R., & Sommaruga, R. (2018). Climate warming increases vertical and seasonal water temperature differences and inter-annual variability in a mountain lake. *Climatic Change*, *151*(3–4), 473–490. https://doi.org/10.1007/s10584-018-2328-6

Nury, A. H., Sharma, A., Mehrotra, R., Marshall, L., & Cordery, I. (2022). Projected changes in the Tibetan Plateau snowpack resulting from rising global temperatures. *Journal of Geophysical Research: Atmospheres*, *127*(6). https://doi.org/10.1029/2021JD036201

Oliver, E. C. J., Benthuysen, J. A., Bindoff, N. L., Hobday, A. J., Holbrook, N. J., Mundy, C. N., & Perkins-Kirkpatrick, S. E. (2017). The unprecedented 2015/16 Tasman Sea marine heatwave. *Nature Communications*, *8*(1), 16101. https://doi.org/10.1038/ncomms16101

O'Reilly, C. M., Alin, S. R., Plisnier, P. D., Cohen, A. S., & Mckee, B. A. (2003). Climate change decreases aquatic ecosystem productivity of Lake Tanganyika, Africa. *Nature*, *424*(6950), 766–768. https://doi.org/10.1038/nature01833

O'Reilly, C. M., Sharma, S., Gray, D. K., Hampton, S. E., Read, J. S., Rowley, R. J., et al. (2015). Rapid and highly variable warming of lake surface waters around the globe. *Geophysical Research Letters*, *42*(10), 773–781. https://doi.org/10.1002/2015GL066235

Paerl, H. W., & Huisman, J. (2008). Blooms like it hot. *Science*, *320*(5872), 57–58. https://doi.org/10.1126/science.1155398

Piccolroaz, S., Toffolon, M., & Majone, B. (2013). A simple lumped model to convert air temperature into surface water temperature in lakes. *Hydrology and Earth System Sciences*, *17*(8), 3323–3338. https://doi.org/10.5194/hess-17-3323-2013

Pilla, R. M., & Williamson, C. E. (2021). Earlier ice breakup induces changepoint responses in duration and variability of spring mixing and summer stratification in dimictic lakes. *Limnology and Oceanography*, *67*(S1), S173–S183. https://doi.org/10.1002/lno.11888

Poole, H. H., & Atkins, W. R. G. (1929). Photo-electric measurements of submarine illumination throughout the year. *Journal of the Marine Biological Association of the United Kingdom*, *16*(1), 297–324. https://doi.org/10.1017/S0025315400029829

Qiao, B. L., Zhu, L. P., & Yang, R. M. (2019). Temporal-spatial differences in lake water storage changes and their links to climate change throughout the Tibetan Plateau. *Remote Sensing of Environment*, *222*, 232–243. https://doi.org/10.1016/j.rse.2018.12.037

Qiu, J. (2008). China: The third pole. *Nature*, *454*(7203), 393–396. https://doi.org/10.1038/454393a

Qiu, Y. B., Guo, H. D., Ruan, Y. J., Shi, L. J., & Tian, B. S. (2017). *A dataset of microwave brightness temperature and freeze-thaw for medium-to-large lakes over the High Asia region 2002-2016*. Science Data Bank. https://doi.org/10.11922/sciencedb.374

Qiu, Y. B., Xie, P. F., Leppärantad, M., Wang, X. X., Lemmetyinen, J., Lin, H., & Shi, L. J. (2019). MODIS-based daily lake ice extent and coverage dataset for Tibetan Plateau. *Big Earth Data*, *3*(2), 170–185. https://doi.org/10.1080/20964471.2019.1631729

Qu, B., Kang, S. C., Chen, F., Zhang, Y. J., & Zhang, G. S. (2012). Lake ice and its effect factors in the Nam Co basin, Tibetan Plateau (in Chinese). *Progressus Inquisitiones De Mutatione Climatis*, *8*(5), 327–333. https://doi.org/10.3969/j.issn.1673-1719.2012.05.003

Richardson, D. C., Filazzola, A., Woolway, R. I., Imrit, M. A., Bouffard, D., Weyhenmeyer, G. A., et al. (2024). Nonlinear responses in interannual variability of lake ice to climate change. *Limnology & Oceanography*, *9999*, 1–13. https://doi.org/10.1002/lno.12527

Rüthrich, F., Reudenbach, C., Thies, B., & Bendix, J. (2015). Lake-Related cloud dynamics on the Tibetan Plateau: Spatial patterns and inter-annual variability. *Journal of Climate*, *28*(23), 9080–9104. https://doi.org/10.1175/JCLI-D-14-00698.1

Schneider, P., & Hook, S. J. (2010). Space observations of inland water bodies show rapid surface warming since 1985. *Geophysical Research Letters*, *37*(22). https://doi.org/10.1029/2010GL045059

Sharma, S., Blagrave, K., Magnuson, J. J., O'Reilly, C. M., Oliver, S., Batt, R. D., et al. (2019). Widespread loss of lake ice around the Northern Hemisphere in a warming world. *Nature Climate Change*, *9*(3), 227–231. https://doi.org/10.1038/s41558-018-0393-5

Sharma, S., & Woolway, I. R. (2021). *Lake ice [in "State of the Climate in 2020"]*. In J. Blunden & T. Boyer (Eds.), *State of the climate in 2020. Bull. Am. Meteorol. Soc.* (pp. S48–S51). https://doi.org/10.1175/2021BAMSStateoftheClimate.1

Shi, Y., Huang, A. N., Ma, W. Q., Wen, L. J., Zhu, L., Wu, Y., et al. (2022). Drivers of warming in Lake Nam Co on Tibetan Plateau over the past 40 years. *Journal of Geophysical Research*, *127*(16). https://doi.org/10.1029/2021JD036320

Song, K. S., Wang, M., Du, J., Yuan, Y., Ma, J. H., Wang, M., & Mu, G. Y. (2016). Spatiotemporal variations of lake surface temperature across the Tibetan Plateau using MODIS LST product. *Remote Sensing*, *8*(10), 854. https://doi.org/10.3390/rs8100854

Steinsberger, T., Schwefel, R., Wüest, A., & Müller, B. (2020). Hypolimnetic oxygen depletion rates in deep lakes: Effects of trophic state and organic matter accumulation. *Limnology & Oceanography*, *65*(12), 3128–3138. https://doi.org/10.1002/lno.11578

Sturm, M., Holmgren, J., König, M., & Morris, K. (1997). The thermal conductivity of seasonal snow. *Journal of Glaciology*, *43*(143), 26–41. https://doi.org/10.3189/s0022143000002781

Su, D. S., Hu, X. Q., Wen, L. J., Lyu, S. H., Gao, X. Q., Zhao, L., et al. (2019). Numerical study on the response of the largest lake in China to climate change. *Hydrology and Earth System Sciences*, *23*(4), 2093–2109. https://doi.org/10.5194/hess-23-2093-2019

Subin, Z. M., Riley, W. J., & Mironov, D. (2012). An improved lake model for climate simulations: Model structure, evaluation, and sensitivity analyses in CESM1. *Journal of Advances in Modeling Earth Systems*, *4*(1), M02001. https://doi.org/10.1029/2011MS000072

Sun, H. B., Feistel, R., Koch, M., & Markoe, A. (2008). New equations for density, entropy, heat capacity, and potential temperature of a saline thermal fluid. *Deep-Sea Research I*, *55*(10), 1304–1310. https://doi.org/10.1016/j.dsr.2008.05.011

Swann, G. E. A., Panizzo, V. N., Piccolroaz, S., Pashley, V., Horstwood, M. S. A., Roberts, S., et al. (2020). Changing nutrient cycling in Lake Baikal, the world's oldest lake. *Proceedings of the National Academy of Sciences*, *117*(44), 27211–27217. https://doi.org/10.1073/pnas.2013181117

Tao, S. L., Fang, J. Y., Ma, S. H., Cai, Q., Xiong, X. Y., Tian, D., et al. (2020). Changes in China's lakes: Climate and human impacts. *National Science Review*, *7*(1), 132–140. https://doi.org/10.1093/nsr/nwz103

Thiery, W., Davin, E. L., Seneviratne, S. I., Bedka, K., Lhermitte, S., & van Lipzig, N. P. M. (2016). Hazardous thunderstorm intensification over Lake Victoria. *Nature Communications*, *7*(1), 12786. https://doi.org/10.1038/ncomms12786

Till, A., Rypel, A. L., Bray, A., & Fey, S. B. (2019). Fish die-offs are concurrent with thermal extremes in north temperate lakes. *Nature Climate Change*, *9*(8), 637–641. https://doi.org/10.1038/s41558-019-0520-y

Tong, K., Su, F. G., & Xu, B. Q. (2016). Quantifying the contribution of glacier meltwater in the expansion of the largest lake in Tibet. *Journal of Geophysical Research*, *121*(19), 11158–11173. https://doi.org/10.1002/2016JD025424

Vavrus, S. J., Wynne, R. H., & Foley, J. A. (1996). Measuring the sensitivity of southern Wisconsin lake ice to climate variations and lake depth using a numerical model. *Limnology & Oceanography*, *41*(5), 822–831. https://doi.org/10.4319/lo.1996.41.5.0822

Verburg, P., Hecky, R. E., & Kling, H. (2003). Ecological consequences of a century of warming in Lake Tanganyika. *Science*, *301*(5632), 505–507. https://doi.org/10.1126/science.1084846

Vinnå, L. R., Medhaug, I., Schmid, M., & Bouffard, D. (2021). The vulnerability of lakes to climate change along an altitudinal gradient. *Communications Earth & Environment*, *2*(1), 35. https://doi.org/10.1038/s43247-021-00106-w

Wan, W., Li, H., Xie, H. J., Hong, Y., Long, D., Zhao, L. M., et al. (2017). A comprehensive data set of lake surface water temperature over the Tibetan Plateau derived from MODIS LST products 2001-2015. *Scientific Data*, *4*(1), 170095. https://doi.org/10.1038/sdata.2017.95

Wan, W., Zhao, L., Xie, H., Liu, B., Li, H., Cui, Y., et al. (2018). Lake surface water temperature change over the Tibetan plateau from 2001 to 2015: A sensitive indicator of the warming climate. *Geophysical Research Letters*, *45*(11), 177–186. https://doi.org/10.1029/2018GL078601

Wang, J., Bai, X. Z., Hu, A. G., Clites, A., Colton, M., & Lofgren, B. (2012). Temporal and spatial variability of Great Lakes ice cover, 1973-2010. *Journal of Climate*, *25*(4), 1318–1329. https://doi.org/10.1175/2011JCLI4066.1

Wang, J., Zhang, M. J., Wang, S. J., Ren, Z. G., Chen, Y. J., Qiang, F., & Qu, D. Y. (2016). Decrease in snowfall/rainfall ratio in the Tibetan Plateau from 1961 to 2013. *Journal of Geographical Sciences*, *26*(9), 1277–1288. https://doi.org/10.1007/s11442-016-1326-8

Wang, J. B. (2020). *Water temperature observation data at Nam Co Lake in Tibet (2011-2014)*. National Tibetan Plateau Data Center. https://doi.org/10.11888/Hydro.tpdc.270332

Wang, M. D., Hou, J. Z., & Lei, Y. B. (2014). Classification of Tibetan lakes based on variations in seasonal lake water temperature. *Chinese Science Bulletin*, *59*(34), 4847–4855. https://doi.org/10.1007/s11434-014-0588-8

Wang, W., Lee, X. H., Xiao, W., Liu, S. D., Schultz, N., Wang, Y. W., et al. (2018). Global lake evaporation accelerated by changes in surface energy allocation in a warmer climate. *Nature Geoscience*, *11*(6), 410–414. https://doi.org/10.1038/s41561-018-0114-8

Wang, X. C., Feng, L., Gibson, L., Qi, W., Liu, J. G., Zheng, Y., et al. (2021). High-resolution mapping of ice cover changes in over 33,000 lakes across the North Temperate Zone. *Geophysical Research Letters*, *48*. https://doi.org/10.1029/2021GL095614.18

Wen, L. J., Nagabhatla, N., Zhao, L., Li, Z. G., & Chen, S. Q. (2015). Impacts of salinity parameterizations on temperature simulation over and in a hypersaline lake. *Chinese Journal of Oceanology and Limnology*, *33*(3), 90–801. https://doi.org/10.1007/s00343-015-4153-3

Weyhenmeyer, G. A., Westöö, A. K., & Willén, E. (2007). *Increasingly ice-free winters and their effects on water quality in Sweden's largest lakes*. In *European Large Lakes Ecosystem Changes and Their Ecological and Socioeconomic Impacts* (pp. 111–118). Springer.

Woolway, R. I., Jennings, E., Shatwell, T., Golub, M., Pierson, D. C., & Maberly, S. C. (2021). Lake heatwaves under climate change. *Nature*, *589*(7842), 402–407. https://doi.org/10.1038/s41586-020-03119-1

Woolway, R. I., Kraemer, B. M., Lenters, J. D., Merchant, C. J., O'Reilly, C. M., & Sharma, S. (2020). Global lake responses to climate change. *Nature Reviews Earth & Environment*, *1*(8), 388–403. https://doi.org/10.1038/s43017-020-0067-5

Woolway, R. I., & Merchant, C. J. (2019). Worldwide alteration of lake mixing regimes in response to climate change. *Nature Geoscience*, *12*(4), 271–276. https://doi.org/10.1038/s41561-019-0322-x

Woolway, R. I., Merchant, C. J., Hoek, J. V. D., Azorin-Molina, C., Nõges, P., Laas, A., et al. (2019). Northern hemisphere atmospheric stilling accelerates lake thermal responses to a warming world. *Geophysical Research Letters*, *46*(21), 11983–11992. https://doi.org/10.1029/2019GL082752

Woolway, R. I., Sharma, S., & Smol, J. P. (2022). Lakes in hot water: The impacts of a changing climate on aquatic ecosystems. *BioScience*, *72*(11), 1050–1061. https://doi.org/10.1093/biosci/biac052

Woolway, R. I., Sharma, S., Weyhenmeyer, G. A., Debolskiy, A., Golub, M., Mercado-Bettín, D., et al. (2021a). Phenological shifts in lake stratification under climate change. *Nature Communications*, *12*(1), 2318. https://doi.org/10.1038/s41467-021-22657-4

Wu, Y., Huang, A. N., Lazhu, Yang, X. Y., Qiu, B., Wen, L. J., et al. (2020). Improvements of the coupled WRF-Lake model over Lake Nam Co, Central Tibetan Plateau. *Climate Dynamics*, *55*(9–10), 2703–2724. https://doi.org/10.1007/s00382-020-05402-3

Wu, Y., Huang, A. N., Yang, B., Dong, G. T., Wen, L. J., Lazhu, et al. (2019). Numerical study on the climatic effect of the lake clusters over Tibetan Plateau in summer. *Climate Dynamics*, *53*(9–10), 5215–5236. https://doi.org/10.1007/s00382-019-04856-4

Wu, Y. H., Guo, L. N., Zhang, B., Zheng, H. X., Fan, L. X., Chi, H. J., et al. (2022). Ice phenology dataset reconstructed from remote sensing and modelling for lakes over the. Tibetan Plateau. *Scientific Data*, *9*(1), 743. https://doi.org/10.1038/s41597-022-01863-9

Xie, C., Zhang, X., Zhuang, L., Zhu, R. X., & Guo, J. (2022). Analysis of surface temperature variation of lakes in China using MODIS land surface temperature data. *Scientific Reports*, *12*(1), 2415. https://doi.org/10.1038/s41598-022-06363-9

Yang, K., Wu, H., Qin, J., Lin, C. H., Tang, W. J., & Chen, Y. Y. (2014). Recent climate changes over the Tibetan Plateau and their impacts on energy and water cycle: A review. *Global and Planetary Change*, *112*, 79–91. https://doi.org/10.1016/j.gloplacha.2013.12.001

Yang, R. M., Zhu, L. P., Wang, J. B., Ju, J. T., Ma, Q. F., Turner, F., & Guo, Y. (2017). Spatiotemporal variations in volume of closed lakes on the Tibetan Plateau and their climatic responses from 1976 to 2013. *Climatic Change*, *140*(3–4), 621–633. https://doi.org/10.1007/s10584-016-1877-9

Yao, T. D., Bolch, T., Chen, D. L., Cao, J., Immerzeel, W., Piao, S. L., et al. (2022). The imbalance of the Asian water tower. *Nature Reviews Earth & Environment*, *3*(10), 618–632. https://doi.org/10.1038/s43017-022-00299-4

Yao, T. D., Xue, Y. K., Chen, D. L., Chen, F. H., Thompson, L., Cui, P., et al. (2019). Recent Third Pole's Rapid warming accompanies cryospheric melt and water cycle intensification and interactions between monsoon and environment: Multidisciplinary approach with

observations, modeling, and analysis. *Bulletin of the American Meteorological Society*, *100*(3), 423–444. https://doi.org/10.1175/BAMS-D-17-0057.1

Yao, X. G., Yang, K., Letu, H., Zhou, X., Wang, Y., Ma, X. G., et al. (2023). Observation and process understanding of typical cloud holes above lakes over the Tibetan Plateau. *Journal of Geophysical Research*, *128*(13). https://doi.org/10.1029/2023JD038617

Yusufova, V. D., Pepinov, R. I., Nikolaev, V. A., & Guseinov, G. M. (1975). Thermal conductivity of aqueous solutions of NaCl. *Journal of Engineering Physics*, *29*(4), 1225–1229. https://doi.org/10.1007/BF00867119

Zhang, G. Q., Bolch, T., Yao, T. D., Rounce, D. R., Chen, W. F., Ven, G., et al. (2023). Underestimated mass loss from lake-terminating glaciers in the greater Himalaya. *Nature Geoscience*, *16*(4), 333–338. https://doi.org/10.1038/s41561-023-01150-1

Zhang, G. Q., Luo, W., Chen, W. F., & Zheng, G. X. (2019). A robust but variable lake expansion on the. Tibetan Plateau. *Science Bulletin*, *64*(18), 1306–1309. https://doi.org/10.1016/j.scib.2019.07.018

Zhang, G. Q., Yao, T. D., Xie, H. J., Qin, J., Ye, Q. H., Dai, Y. F., & Guo, R. F. (2014). Estimating surface temperature changes of lakes in the Tibetan Plateau using MODIS LST data. *Journal of Geophysical Research: Atmospheres*, *119*(14), 8552–8567. https://doi.org/10.1002/2014JD021615

Zhang, G. Q., Yao, T. D., Xie, H. J., Yang, K., Zhu, L. P., Shum, C. K., et al. (2020). Response of Tibetan Plateau lakes to climate change: Trends, patterns, and mechanisms. *Earth-Science Reviews*, *208*, 103269. https://doi.org/10.1016/j.earscirev.2020.103269

Zhang, Y. L., Wu, Z. X., Liu, M. L., He, J. B., Shi, K., Zhou, Y. Q., et al. (2015). Dissolved oxygen stratification and response to thermal structure and long-term climate change in a large and deep subtropical reservoir (Lake Qiandaohu, China). *Water Research*, *75*, 249–258. https://doi.org/10.1016/j.watres.2015.02.052

Zhao, G., Li, Y., Zhou, L. M., & Gao, H. L. (2022). Evaporative water loss of 1.42 million global lakes. *Nature Communications*, *13*(1), 3686. https://doi.org/10.1038/s41467-022-31125-6

Zhong, Y. F., Notaro, M., Vavrus, S. J., & Foster, M. J. (2016). Recent accelerated warming of the Laurentian Great Lakes: Physical drivers. *Limnology & Oceanography*, *61*(5), 1762–1786. https://doi.org/10.1002/lno.10331

Zhu, L. P. (2021). In-situ water quality parameters of the lakes on the Tibetan Plateau (2009-2020). [Dataset]. *National Tibetan Plateau Data Center*. https://doi.org/10.11888/Geogra.tpdc.271450